CORROSION OF ALLOY 22 AND TITANIUM ALLOYS UNDER SEEPAGE WATER DRIPPING CONDITION

Prepared for

U.S. Nuclear Regulatory Commission
Contract NRC–02–07–006

Prepared by

Hundal Jung[1]
Xihua He[1]
Tae Ahn[2]
Todd Mintz[1]
Roberto Pabalan[1]

[1]Center for Nuclear Waste Regulatory Analyses
San Antonio, Texas

[2]U.S. Nuclear Regulatory Commission
Washington, DC

September 2011

ABSTRACT

This report documents the results of a previously unpublished set of experiments that evaluated the corrosion behavior of Alloy 22 and titanium alloys (Grades 7 and 29) under seepage water dripping conditions at controlled temperature and relative humidity. Tests were conducted inside a chamber with controlled temperature and relative humidity. The simulated seepage water was dripped on the test specimens at rates of 65 or 80 mL/day [2.20 or 2.71 oz/day] depending on the test temperature. Three batches of tests were conducted for Alloy 22: a first batch at 80 °C [176 °F] and 85 percent relative humidity, a second batch at 95 °C [203 °F] and 75 percent relative humidity, and a third batch at 60 °C [140 °F] and 95 percent relative humidity. The first two batches of tests were conducted for titanium alloys. After testing, the posttest specimens were examined with an optical microscope and salt deposits were analyzed in terms of chemical composition and crystal structure. Finally, after cleaning the posttest specimens, weight loss was measured to calculate corrosion rates of Alloy 22 and titanium alloys.

In all of the tested conditions for Alloy 22, white deposits were observed on the posttest specimens. In the first batch of tests, the surfaces of the posttest specimens exhibited several corrosion pits along with many small sized pits ranged about 1 to 10 μm [3.94×10^{-5} to 3.94×10^{-4} in] after 35 days of the dripping test. After 185 days of testing, however, the pits appeared to be shallow and there was no clear evidence of pit propagation. The corrosion rate decreased with test duration, and the rate measured after 185 days' exposure was 25 nm/yr [9.84×10^{-7} in/yr]. In the second batch at 95 °C [203 °F], pits were also present on the specimen surface. However, with time, the corrosion rate decreased. At the low temperature of 60 °C [140 °F] and the relative humidity of 95 percent, the corrosion rate decreased with time and was 24 nm/yr [9.45×10^{-7} in] after 60 days of testing. There was no evidence of pit propagation. Under the seepage water dripping condition, Alloy 22 exhibited a temperature-dependent corrosion rate, which was commonly observed in the immersion tests. The corrosion rates obtained from the dripping tests in this study were close to the rates obtained from the immersion tests in the literature. Results of the salt chemistry analyses through thermodynamic calculations and analysis tools indicate that the major composition was calcium carbonate and other several compositions were also precipitated, including magnesium carbonate, sodium (calcium) sulfate, sodium chloride, and silica.

For Titanium Grades 7 and 29 materials, the first batch of tests at 80 °C [176 °F] and 85 percent relative humidity for 181 days showed that the corrosion rates of the specimens subjected to dripping were in the range of 20–50 nm/yr [7.9×10^{-7}–2.0×10^{-6} in/yr], similar to the rates reported in the literature obtained from immersed conditions in similar water chemistry. No clear difference was observed between Titanium Grades 7 and 29. The front side surface subjected to direct dripping corroded more than the back side that was not subjected to direct dripping. The second batch of tests at 95 °C [203 °F] and 75 percent relative humidity for 64 days showed that the corrosion rates for Titanium Grades 7 and 29 under dripping were 130–380 nm/yr [5.12×10^{-6}–1.50×10^{-5} in/yr] and 260–530 nm/yr [1.02×10^{-5}–2.09×10^{-5} in/yr], respectively; higher than what was measured from the first batch of tests. The higher corrosion rates could be caused by the shorter test duration and higher test temperature. No localized corrosion was observed on either titanium alloys from the two batches of tests.

CONTENTS

FIGURES

FIGURES (continued)

TABLES

ACKNOWLEDGMENTS

QUALITY OF DATA, ANALYSES, AND CODE DEVELOPMENT

DATA: All CNWRA-generated original data contained in this report meet the quality assurance requirements described in the Geosciences and Engineering Division Quality Assurance Manual. Sources for other data should be consulted for determining the level of quality for those data. All data and calculations related to this report have been recorded in CNWRA Scientific Notebook 899 (Jung, et al., 2011) for Alloy 22 and Scientific Notebook 1024E (He, 2011) for titanium alloys.

ANALYSES AND CODES: The computer software OLI Analyzer Studio Version 3 code (Gerbino, 2006; OLI Systems, Inc., 2010) was used for the analyses contained in this report. This software is commercial software controlled under the CNWRA quality assurance procedure Technical Operating Procedure (TOP)–18.

References

Gerbino, A. "A Guide for Using the OLI Analyzers." Morris Plains, New Jersey: OLI Systems, Inc. 2006.

He, X. "Corrosion Tests of Titanium Alloys and Borated Stainless Steel." Scientific Notebook No. 1024E. San Antonio, Texas: CNWRA. pp. 1–68. 2011.

Jung, H., B. Derby, and G. Bird. "Seepage Water Dripping Test for Alloy 22 in the Repository Relevant Environments." Scientific Notebook No. 899. San Antonio, Texas: CNWRA. pp. 1–107. 2011.

OLI Systems, Inc. "A Guide to Using OLI Analyzer Studio Version 3.1." Morris Plains, New Jersey: OLI Systems, Inc. 2010.

1   INTRODUCTION

This report is part of the knowledge management activities for the U.S. Nuclear Regulatory Commission high-level waste repository safety program. The report provides previously undocumented results from recent corrosion tests that used weight loss measurements and surface analysis to evaluate the corrosion behaviors of Alloy 22 and titanium alloys under seepage water dripping conditions. The corrosion experiments were conducted by dripping simulated seepage water in three batches with varying temperature and relative humidity: a first batch at 80 °C [176 °F] and 85 percent relative humidity, a second batch at 95 °C [203 °F] and 75 percent relative humidity, and a third batch at 60 °C [140 °F] and 95 percent relative humidity. The corrosion rates of Alloy 22 and titanium alloys were estimated by measuring weight loss of the posttest specimens. The surface of the specimen was examined with an optical microscope, and the salts deposited on the specimen were also analyzed using energy dispersive x-ray spectroscopy (EDS) and x-ray diffraction (XRD).

1.1   Background Information

Alloy 22 (Ni−22Cr−13Mo−3W−4Fe) and titanium alloys (Grade 7 and 29) have been candidates for the waste package outer container and drip shield materials, respectively, in the proposed Yucca Mountain repository (Sandia National Laboratories, 2007a,b). These materials have also been studied in various disposal programs around the world as reference waste package materials in various geological settings due to their high corrosion resistance (Kursten et al., 2004). The high corrosion resistances of Alloy 22 and titanium alloys are attributed in part to the presence of passive films that protect against fast corrosion. In the event of deterioration or loss of passivity of these alloys, they can fail by fast corrosion. Therefore, it is important to determine the long-term corrosion rate and susceptibility to localized corrosion of these alloys under various service conditions.

Most corrosion data on these alloys used in the disposal program were obtained from immersion experiments to develop the model abstraction for general corrosion rate and susceptibility to localized corrosion. In an unsaturated disposal environment, however, the corrosion conditions may include dripping seepage water contacting the waste package containers (Sandia National Laboratories, 2007a). In addition, the container temperatures would be higher than ambient values due to radioactive decay. Therefore, it is expected that salt deposits can form on surfaces by seepage water evaporation.

Environmental Conditions of Temperature, Relative Humidity, and Water Dripping Rate in This Study

Figures 1-1 and 1-2 show the modeled ranges of temperature and relative humidity versus time for all waste packages in the proposed Yucca Mountain repository, accounting for uncertainty of host-rock thermal conductivity and percolation flux (Sandia National Laboratories, 2008a). During the first 10,000 years, the waste package temperatures could have a wide range, from a peak of 203 °C [398 °F] to room temperature. In the time period of 1,500 and 10,000 years, there is a possibility that one or a few drip shields could fail by seismic impact, allowing seepage water to contact the waste package (Sandia National Laboratories, 2008a). During this period, the average temperature could range from about 95 to 60 °C [203 to 140 °F] and the average relative humidity could range from approximately 75 to 95 percent. These ranges of modeled temperature and relative humidity were selected for the experimental conditions in this study.
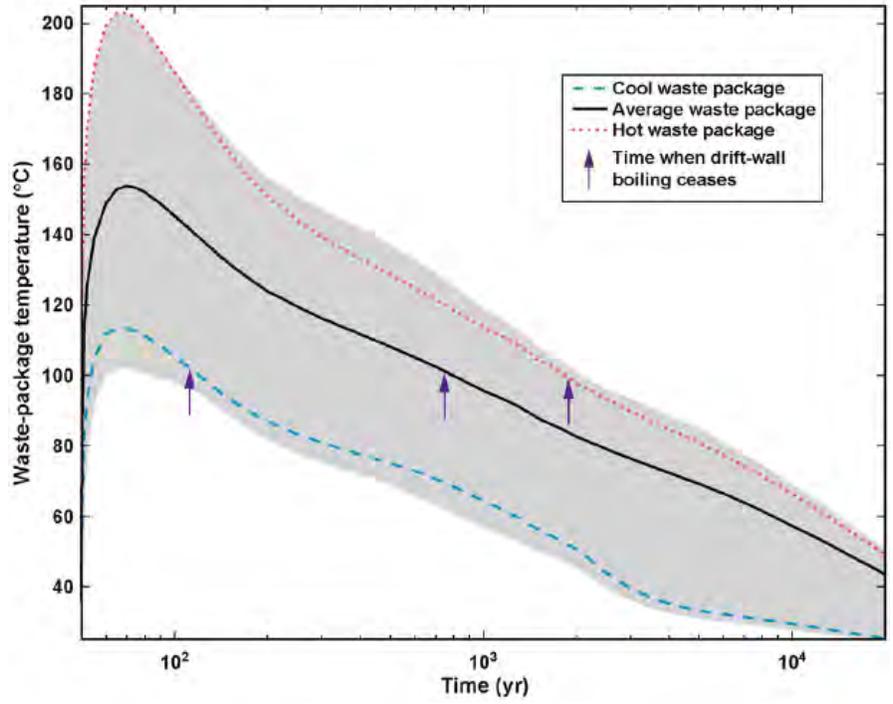
Figure 1-1. Range of Modeled Waste Package Temperature Versus Time in the Yucca Mountain Performance Assessment (Sandia National Laboratories, 2008a)
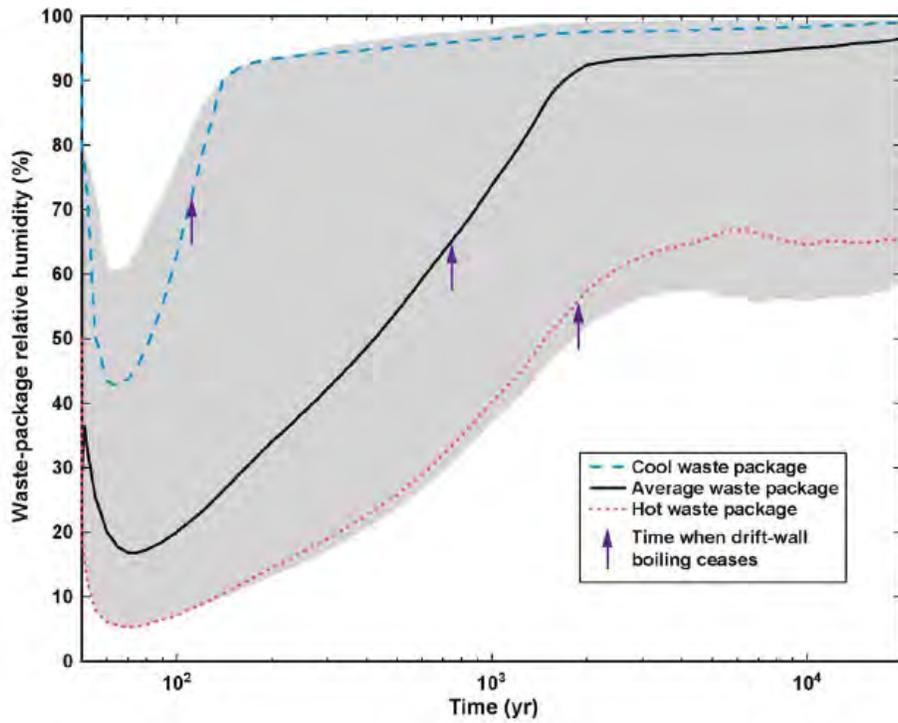
Figure 1-2. Range Modeled of Relative Humidity Versus Time in the Yucca Mountain Performance Assessment (Sandia National Laboratories, 2008a)

The water dripping rates for the dripping tests in this study were selected based on the modeled seepage water flow rates as a function of repository time (Sandia National Laboratories, 2008b) and adjusted to have a focused flow to the test specimen because the seepage water dripping will not be uniform (i.e., not evenly distributed onto either the drip shield surface from the drift wall or the waste package surface from the breached areas of the drip shield). Lin, et al. (2003) calculated the dripping rate of seepage water to the waste package when the flow was focused through the breached area of the drip shield. They found that the dripping rates could increase 100 to 10,000 times, depending on the size of the focused area. Therefore, in this study, the dripping rate was also adjusted to be either 65 or 80 mL/day [2.20 or 2.71 oz/day], depending on the test temperature. Scaling from the surface area of 0.002 m^2 [3.10 in^2] of the Alloy 22 test sample to the surface area of 33 m^2 [51,150 in^2] of one waste package, these rates are equivalent to 360,000 to 482,000 kg/yr [7.94 × 10^5 to 1.06 × 10^6 lb/yr] with a focusing factor of ~1,100. In the literature, the dripping rates used for Alloy 22 were about 30 mL/day [1.01 oz/day] of simulated concentrated water (Ashida, et al., 2008) or 200 mL/day [6.76 oz/day] of simulated seepage water (Dunn, et al., 2006). The rates in this study fall between these two rates, which is a good range to compare the test results with the literature results.

Dripping Water Droplet Size

The volume (mass) of water droplets in the experiments was initially estimated by a mass balance between gravitational force and capillary force by surface tension. Assuming a spherical water drop, the gravitational energy per unit volume from the mass of half of a spherical water droplet is

$$\rho \times g \times R \quad [\text{erg/cm}^3] \tag{1-1}$$

where ρ is density of water {e.g., 1 g/cm^3 [3.56 × 10^{-2} lb/in^3] for pure water, varying with dissolved species}; g is gravitational force {980 cm/sec^2 [385.8 in/sec^2]}; and R is the radius of the droplet. The surface energy per unit volume due to surface tension of the droplet is

$$2 \times \gamma_m/R \quad [\text{erg/cm}^3] \tag{1-2}$$

where γ_m is specific surface energy of the drop e.g., ~100 erg/cm^2 [645.2 erg/in^2] for pure water, varying with dissolved species and substrates. By equating these two terms, R is calculated to be ~0.45 cm [0.177 in]. If the drop is bigger than this size, it will flow on the waste package surface or on the drift wall surface. The mass of half of a spherical droplet is 0.19 g [6.7 × 10^{-3} oz].

This value was different from the actual measured mass of one water droplet. The measured mass of a water droplet in this study was about 0.075 g [2.65 × 10^{-3} oz]. This actual measured mass was used to adjust the water dripping frequency to be either 65 or 80 mL/day [2.20 or 2.71 oz/day] in this study. This is presumably due to the complex, nonspherical nature of a water drop, affected by aqueous water chemistry or temperature, or by the gravitational force on the necking of the drop. The total volume of the half sphere may not drop completely, because a portion of the droplet water will remain on the rock surface.

1.2 Objective and Organization of the Report

The objective of this report is to document the results of recent corrosion tests that used weight loss measurements and surface analysis to evaluate the corrosion behavior of Alloy 22 and titanium alloys under seepage water dripping conditions. The corrosion tests were conducted to

assess the persistence of the passive film and to measure the corrosion rate. The persistence of the passive film was assessed by determining susceptibility to localized corrosion (primarily pitting), and the corrosion rate was determined by weight loss measurement. Note that this report presents preliminary results; longer term corrosion tests are warranted for conclusive results.

This report consists of four chapters: introduction, experimental details, results and discussion, and conclusions. This chapter briefly describes the corrosion behaviors of Alloy 22 and titanium alloys. Environmental conditions including temperature, relative humidity, and seepage water dripping rates under seepage water dripping conditions in a repository are also discussed in this chapter. Experimental conditions in this study are provided in Chapter 2, including details of test samples, test solutions, and test procedures. Relative humidity, water droplet size, and frequency of dripping were controlled, in addition to temperature and seepage water chemistry. The values of these variables used in the test are detailed in Chapter 2. Results of experiments and analyses are discussed in Chapter 3, including surface and salt analyses, weight loss measurements, and corrosion rate calculations. Chapter 4 presents the study conclusions.

2   EXPERIMENTAL DETAILS

2.1   Materials

2.1.1   Alloy 22 Sheet

The samples used for the tests were disk-shaped Alloy 22 sheet metal. The chemical composition of the Alloy 22 (HT 2277–9–3119) samples is shown in Table 2-1. The samples had a diameter of 5.08 cm [2.0 in] and a thickness of 0.0635 cm [0.025 in]. The specimens were polished using up to a 2,000-grit sandpaper and 2,000 diamond paste for final finish, rinsed and ultrasonically cleaned in deionized water and acetone, and dried.

2.1.2   Titanium Alloys

Titanium Grades 7 and 29 coupons with approximate dimensions of $4 \times 4 \times 0.6$ cm^3 [$1.6 \times 1.6 \times 0.2$ in^3] were used in the dripping tests. The Titanium Grade 7 specimens were sectioned from the middle of a 1.27-cm [0.5-in]-thick Titanium Grade 7 plate as schematically shown in Figure 2-1(a). Because of the unavailability of Titanium Grade 29 plate, the Titanium Grade 29 specimen was machined from the wall of a seamless extruded pipe {40 cm [16 in] outer diameter and 1.4-cm [0.57-in] wall thickness} obtained from Titanium Metals Corporation as shown in Figure 2-1(b). The Titanium Grade 7 is in mill-annealed condition with single α-phase conforming to ASTM B265 (ASTM International, 2008). The Titanium Grade 29 pipe is in the β-transformed (final processed above the β-transus temperature) plus subsequently annealed condition conforming to ASTM B861 (ASTM International, 2010). The microstructures of the two materials are shown in Figure 2-2. The chemical composition of the titanium specimens used in this study is shown in Table 2-2. The specimens were polished with 120-, 240-, 320-, 400-, 600-, 1,000-, 2,000-grit sandpaper and 2,000 diamond paste, and 1-μm alumina suspension for final finish; rinsed and ultrasonically cleaned in deionized water and acetone; and dried.

2.2   Test Procedures

The dripping corrosion tests of Alloy 22 and titanium alloys were conducted inside a chamber with a controlled temperature and relative humidity as shown in Figure 2-3. Each test specimen was set on a 3.4 cm [1.3 in] outer diameter polytetrafluoroethylene (PTFE) cylinder spacer. The PTFE cylinders with the test specimens were placed inside a PTFE tray in the chamber. The top of the dripping tubes was located about 10 cm [3.94 in] above the test specimen. The dripping water is simulated seepage water with the chemical composition shown in Table 2-3. Dunn, et al. (2006) used the same composition to represent neutral-type seepage waters in experiments to evaluate the effect of environmental conditions on the performance of the Alloy 22 waste package material. The water was pumped from a reservoir outside of the chamber through PTFE tubing into the chamber and allowed to drip on the test specimens. The temperature and relative humidity were controlled and maintained constant through the testing periods. The temperature and relative humidity near the test specimens were monitored by using additional measurement probes from the outside. The probes of the thermocouple and humidity gauge were extended to be located close to the test specimens. Because the temperature and humidity sensors were located at the edge of the ceiling inside the chamber, it was necessary to confirm the actual temperature and relative humidity to which the test specimens located on the floor inside the chamber were directly exposed.

Table 2-1. Chemical Composition of Mill-Annealed Alloy 22 (in Weight Percent)												
Ni*	Cr*	Mo*	W*	Fe*	Co*	Si*	Al*	Mn*	V*	P*	S*	C*
Bal†	21.62	12.98	2.86	3.56	1.29	0.03	0.22	0.29	0.01	0.008	0.0005	0.004

*Ni—nitrogen; Cr—chromium; Mo—molybdenum; W—tungsten; Fe—iron; Co—cobalt; Si—silicon;
 Al—aluminum; Mn—manganese; V—vanadium; P—phosphorous; S—sulfur; C—carbon
†Bal—balance
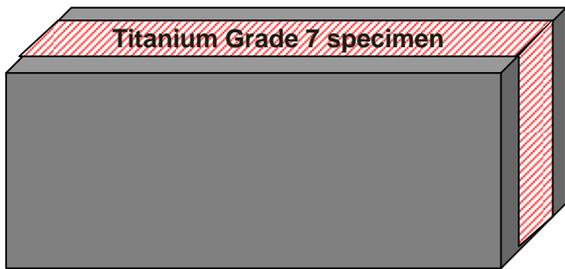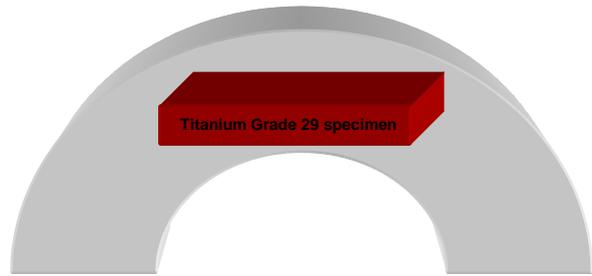
(a)   (b)

Figure 2-1. (a) Titanium Grade 7 and (b) Titanium Grade 29 Specimens Machined From Original Plate or Pipe Sections
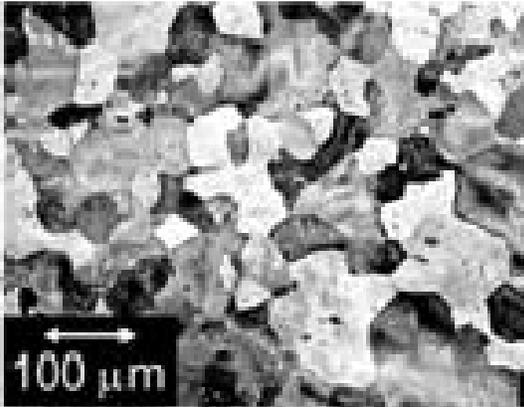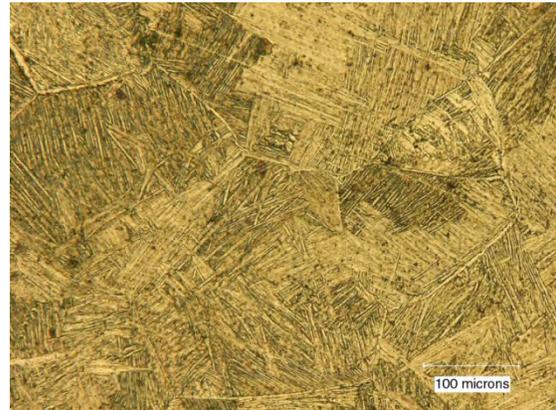
(a) Titanium Grade 7   (b) Titanium Grade 29

Figure 2-2. Microstructure of (a) Titanium Grade 7 and (b) Titanium Grade 29 Specimens

Table 2-2. Chemical Composition of Titanium Grades 7 and Grade 29 (in Weight Percent)										
Material	Ti*	Pd*	Fe*	C*	N*	O*	H*	Al*	V*	Ru*
Titanium Grade 7 Heat CN2775	Bal.	0.16	0.08	0.01	0.01	0.13	0.001	NA	NA	NA
Titanium Grade 29 Heat 00192DB	Bal.	NA	0.19	0.04	0.006	0.109	0.0021	5.62	4.16	0.10

*Ti—titanium, Pd—palladium, Fe—iron, C—carbon, N—nitrogen, O—oxygen, H—hydrogen, Al—aluminum, V—vanadium, Ru—ruthenium
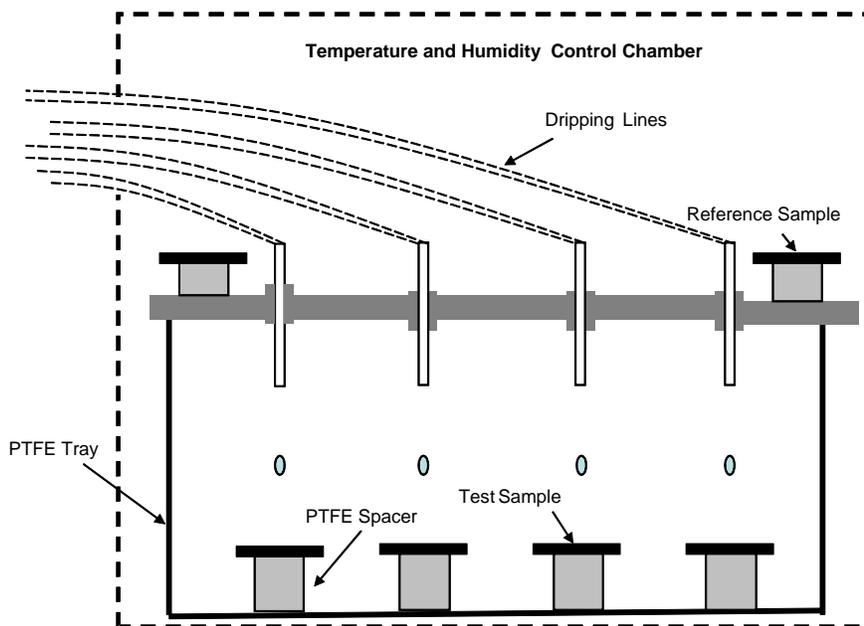
Figure 2-3. Experimental Setup For Dripping Test

Table 2-3. Chemical Composition of Simulated Seepage Water in This Study									
Ion	Na^+	K^+	Mg^{2+}	Ca^{2+}	Cl^-	SO_4^{2-}	NO_3^-	HCO_3^-	CO_3^{2-}
mol/L (M)	1.5×10^{-2}	1.7×10^{-4}	4.9×10^{-4}	9.9×10^{-4}	7.7×10^{-4}	7.0×10^{-3}	1.5×10^{-3}	1.7×10^{-3}	1.7×10^{-5}

The posttest specimens were observed under optical microscope for pitting or other possible corrosion features. Surface deposits and/or surface oxides on the posttest specimens were analyzed with EDS and XRD. Weight loss measurement was used to measure the corrosion rates of Alloy 22 and titanium alloys.

2.2.1 Test Procedures for Alloy 22

In all of the tested conditions for Alloy 22, white deposits were observed on the surface of posttest specimens. After carefully removing and collecting the surface deposits, the specimens were first rinsed with deionized water and then chemically cleaned multiple times in an HCl solution {150 mL [5.1 oz] diluted to 1,000 mL [34 oz] deionized water} in accordance with the procedures recommended in ASTM G1–03 (ASTM International, 2003). The specimens were immersed and agitated for 2 minutes at room temperature. Then, the specimens were ultrasonically cleaned in acetone and dried. Before measuring the weight loss of the posttest specimens, the cleaned surface was observed by optical microscope to confirm the absence of any remaining deposits on the surface. The weight change was measured using a microbalance with a precision of $\pm 2.5 \times 10^{-5}$ g [8.82×10^{-7} oz]. Figure 2-4 shows a typical plot for weight loss measurements as a function of the number of cleanings. The four test specimens were exposed at 80 °C [176 °F] and 85 percent relative humidity for 35 days. Most of the weight loss plateaued after two or three cycles of cleaning. Therefore, the weight losses after the third cycle of cleaning were used to calculate the corrosion rate in accordance with the equation defined in ASTM G1–03 (ASTM International, 2003).

Table 2-4 shows the test matrix of Alloy 22 including three batches of temperature and humidity: a first batch at 80 °C [176 °F] and 85 percent relative humidity, a second batch at 95 °C [203 °F] and 75 percent relative humidity, and a third batch at 60 °C [140 °F] and 95 percent relative humidity. The table also provides information on the test duration and sample identification number for each batch. The water dripping rates for each set were selected and adjusted to be a focused flow equivalent to the test specimen size, as discussed in Chapter 1. The droplet size was also discussed in Chapter 1.

To evaluate the depth of pitting, four specimens were analyzed with a laser profilometer. These included two Alloy 22 samples held at 80 °C [176 °F] for 35 days (specimens A and B) and another two samples held at the same temperature for 185 days (specimens G and H). The laser profilometer is a noncontact, fully automatic imaging system with a depth resolution (z-axis of the machine) of 0.5 μm [1.97×10^{-5} in] and lateral surface resolution of 1 μm [3.94×10^{-5} in] (x- and y-axes). The laser profilometer uses a laser-optical displacement sensor and signal conditioning electronics to measure the vertical distance on a material. The laser used is a helium-neon laser operating a wavelength of 632.8 nm. The sensor uses the optical
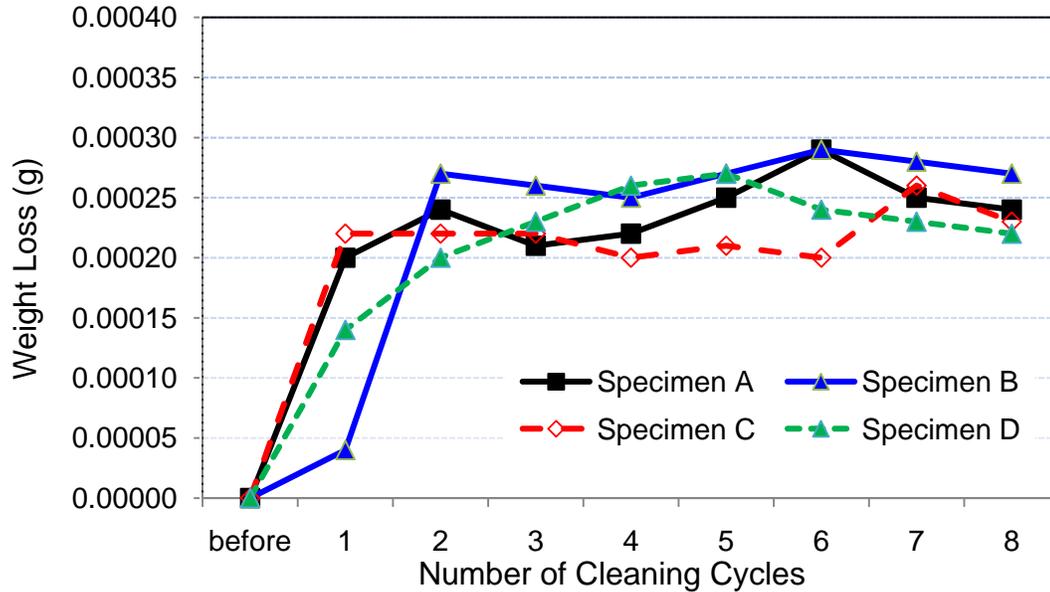
Figure 2-4. Weight Losses of the Corroded Test Specimens Resulting From Repetitive Cleaning Cycles in an ASTM HCl Solution (ASTM International, 2003). The Weight Loss After the Third Cycle of Cleaning Was Used in the Weight Loss Analysis.

Table 2-4. Test Matrix of Alloy 22 Dripping Tests			
Temperature and Relative Humidity	**Water Dripping Rate**	**Test Duration**	**Specimen Identification**
80 °C [176 °F] and 85 Percent Relative Humidity	80 mL/day [2.71 oz/day]	35 Days	A, B, C, and D
		70 Days	E and F
		185 Days	G and H
95 °C [203 °F] and 75 Percent Relative Humidity	65 mL/day [2.20 oz/day]	33 Days	I and J
		67 Days	K and L
60 °C [140 °F] and 95 Percent Relative Humidity	80 mL/day [2.71 oz/day]	32 Days	M, N, O, and P
		60 Days	Q and R

triangulation principle where a visible, modulated point of light is projected onto the sample surface. The diffusive part of the reflection of this point of light is focused onto a charged, coupled device array. The intensity of the beam provides information about the vertical distance. Laser scans of surface morphology were conducted for all four samples. The scan lateral resolution was set at 5 μm [1.97×10^{-4} in]. The scan of the pit was initiated and ended on the surface of the samples that were only degraded by general corrosion.

2.2.2 Test Procedures for Titanium Alloys

As schematically shown in Figure 2-3, dripping tests of titanium alloys were conducted inside the same chamber with the same setup as for Alloy 22. Each titanium coupon was set on a 3.4 cm [1.3 in] outer diameter PTFE cylinder with one 4 × 4-cm [1.6 × 1.6-in] side subject to dripping. For the first batch of tests at 80 °C [176 °F] and relative humidity of 85 percent with a test duration of 181 days, 2 coupons for each material were subject to dripping. The dripping rate was approximately 80 mL/day [2.7 oz/day] as shown in Table 2-4. The droplet size was discussed in Chapter 1. For the second batch of tests at 95 °C [203 °F] and relative humidity of 75 percent with a test duration of 64 days, 3 coupons for each material were used for dripping. The dripping water is simulated seepage water, which is the same as that for Alloy 22. For each batch of tests, one additional coupon for each material without dripping was set in the chamber under the same temperature and relative humidity as the reference specimen for comparison.

Weight loss measurement was used to measure the corrosion rate. After testing, the coupons were rinsed with deionized water, ultrasonically cleaned, dried, and weighed. The coupons were observed under microscope for pitting or other possible corrosion features. Surface deposits and surface oxides were analyzed with EDS. Afterwards the coupons were chemically cleaned multiple times using cleaning procedures in ASTM G1–03 (ASTM International, 2003) as a guidance. ASTM G1–03 (ASTM International, 2003) did not recommend a solution recipe to clean titanium. The recipe used in this work was obtained from that used in the literature for Titanium Grade 7 (Bechtel SAIC Company LLC, 2004). The coupons were cleaned for 2 minutes at room temperature in the solution prepared by diluting 150 mL [5.07 oz] of concentrated HCl acid (37.0 percent HCl of specific gravity of 1.19) with deionized water to 1,000 mL [33.8 oz] of solution. During each cleaning, one new coupon without any corrosion testing, but with the same surface finish as the test specimen, was cleaned as a control specimen along with the corroded specimen. After each cleaning, the specimen was ultrasonically cleaned in deionized water, then dried and weighed.

3 RESULTS AND DISCUSSION

This section summarizes and discusses the results of experiments and analyses of Alloy 22 and titanium alloys including weight loss measurements and corrosion surface morphologies. In addition, salt deposits formed on the posttest specimens were characterized in terms of chemical composition and crystal structure using EDS and XRD.

3.1 Alloy 22 Dripping Test

Three batches of Alloy 22 dripping tests were conducted: a first batch at 80 °C [176 °F] and 85 percent relative humidity, a second batch at 95 °C [203 °F] and 75 percent relative humidity, and a third batch at 60 °C [140 °F] and 95 percent relative humidity.

3.1.1 First Batch of Tests at 80 °C [176 °F] and Relative Humidity of 85 Percent

Figure 3-1 shows the optical photos of the posttest specimens after 35, 70, and 185 days of the dripping tests at 80 °C [176 °F] and relative humidity of 85 percent. Most of the surface areas on the front upper side subjected to water dripping were covered with white salt deposits. The white deposits were also observed on the lower side, particularly the outside area of the PTFE spacer covered inner area as seen in Figure 3-1(f).

Optical Microscopy

After removing the salt deposits, followed by sample cleaning with HCl solutions, the specimens were examined with an optical microscope. Figure 3-2 shows typical morphologies of the corroded surface of Alloy 22. After 35 days of the dripping test, as shown in Figure 3-2(a), corrosion pits were observed throughout the area exposed to the dripping water. Many small sized pits ranged about 1 to 10 μm [3.94×10^{-5} to 3.94×10^{-4} in] were also present. With dripping for 70 days, as shown in Figure 3-2(b), the surface exhibited similar pits in terms of pit size and popularity. However, pitting appeared to a lesser extent, indicating no growth of nucleated pits. After longer term tests (185 days) the pits appeared to be smaller and shallow. There was no clear evidence of pit propagation. Ashida, et al. (2008) also observed salt deposit formation and localized corrosion (i.e., pitting and intergranular corrosion) on the Alloy 22 surface after 40 days' dripping of saturated concentrated water at 90 °C [194 °F]. However, the microsized pits were not stable and did not grow deep. A similar observation was reported on Alloy 22 tested in saturated acidic water at 80 °C [176 °F] (Badwe, et al., 2006).

Surface Topography

The pits were further analyzed by using a laser profilometer to estimate the pit depth. Figure 3-3(a) shows the typical pit morphology of the corroded surface of Alloy 22 after 35 days' exposure to dripping conditions. As can be seen from both the three-dimensional (3-D) and two-dimensional (2-D) profiles in Figure 3-3(b,c) the pit has a width of roughly 150 μm [5.91×10^{-3} in], with a depth of roughly 40 μm [1.58×10^{-3} in]. These results are similar to those observed from the optical microscopy. Figures 3-4(a) shows the typical pit morphology of the corroded surface of Alloy 22 after 185 days' exposure to the dripping water. Figure 3-3(a) and 3-4(a) are taken at the same magnification. As can be seen from Figure 3-4(a), the pit morphology is not much different from that after 35 days. Figure 3-4(b,c) shows the 2-D and 3-D profiles for the 185-day exposed pit. The pit width is roughly 125 μm [4.92×10^{-3} in], with a
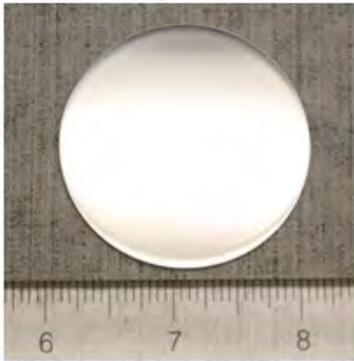
(a)

(b)

(c)
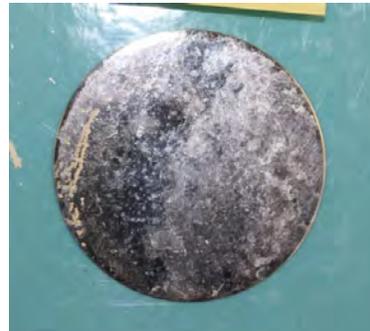
(d)
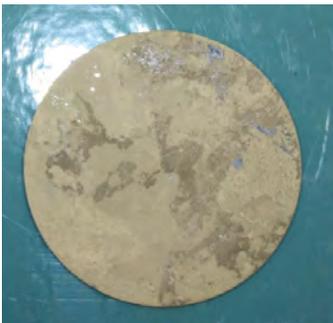
(e)
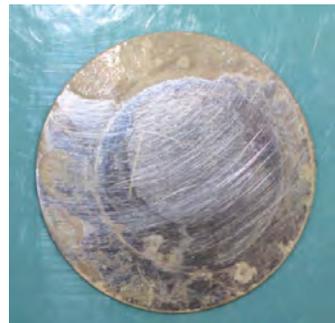
(f)

Figure 3-1. Photos of Pre- and Posttest Surfaces of Alloy 22 Tested at 80 °C [176 °F] and 85 Percent Relative Humidity: (a) Before Corrosion Test, (b) Chamber Inside During Dripping, (c) After 35 Days Dripped, (d) After 70 Days Dripped, (e) After 185 Days Dripped (Upper Side), and (f) After 185 Days Dripped (Lower Side)
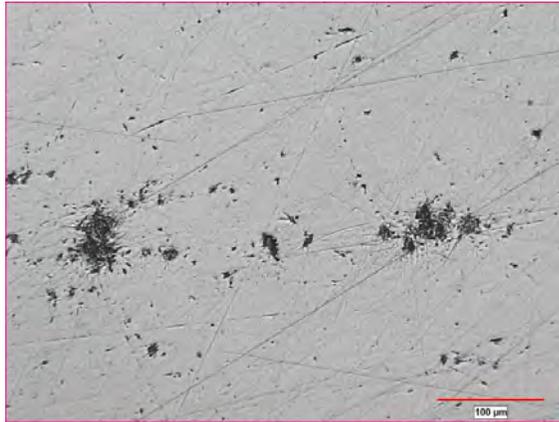
(a)
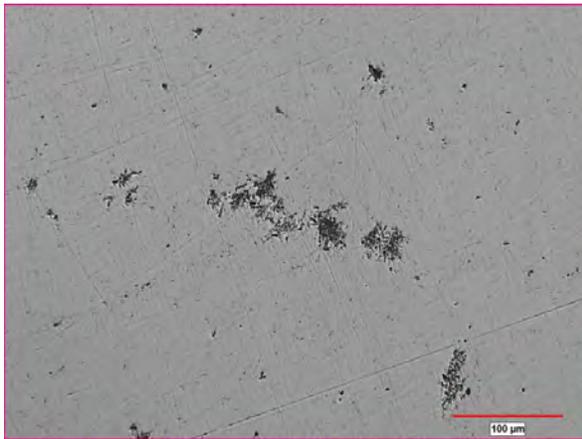
(b)

(c)

Figure 3-2. Optical Micrographs of Alloy 22 Surfaces Tested at 80 °C [176 °F] and 85 Percent Relative Humidity: (a) After 35 Days Dripped, (b) After 70 Days Dripped, and (c) After 185 Days Dripped

depth roughly 30 μm [1.18 × 10^{-3} in]. Similar to the results observed from the optical microscopy, there was no evidence of pit propagation.

Corrosion Rate as a Function Time

Corrosion rates of Alloy 22 specimens were calculated using Eq. (3-1) per ASTM G1–03 (ASTM International, 2003), and results are listed in Table 3-1.

$$\text{Corrosion Rate [nm/yr]} = (8.76 \times 10^{10} \times \Delta w) / (\rho \times A \times t) \qquad (3\text{-}1)$$

where Δw id weight loss (g), ρ is Alloy 22 density {8.69 g/cm^3 [0.31 lb/in^3]}, A is exposed surface area {32.47 cm^2 [5.03 in^2]}, and t is exposed time (hours). The exposed surface of 32.47 cm^2 [5.03 in^{-2}] is the sum of the areas including the front side surface of 20.27 cm^2 [3.14 in^2], the edge area of 1.01 cm^2 [0.16 in^2], and the wetted back side surface of 11.19 cm^2 [1.73 in^2].

(a)
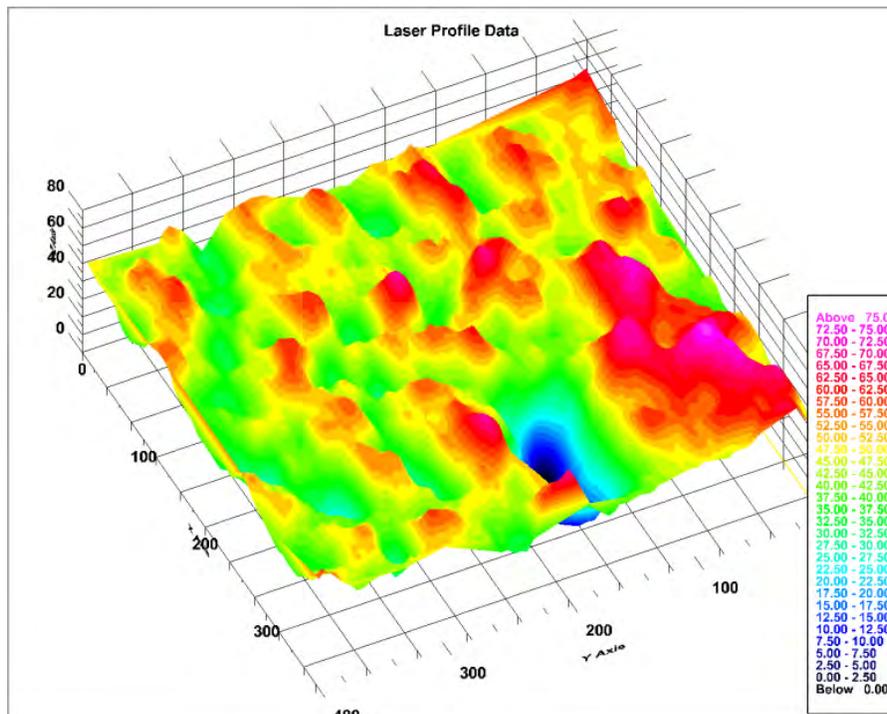
(b)

Figure 3-3. Surface Topography of Alloy 22 Specimen After 35 Days Dripped at 80 °C [176 °F] and 85 Percent Relative Humidity: (a) Optical Micrograph, (b) 3-D Laser Scan Profiles of the Pit Area, and (c) 2-D Profiles

Note: The Square Box in (a) Indicates the Laser Scanning Area.

The Units in (b) and (c) Indicate x-, y-, z-axes Are Micrometer.

Laser Line Profile Data
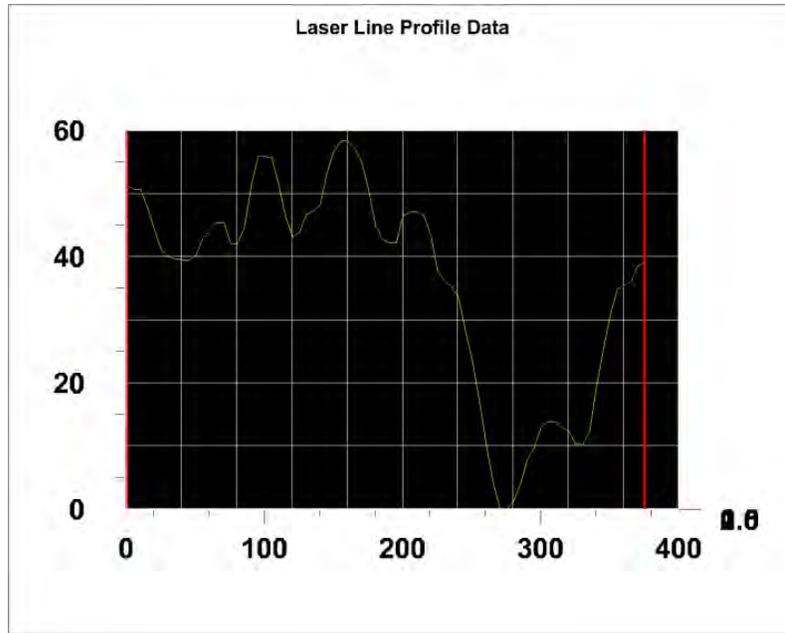
(c)

Figure 3-3 (continued). Surface Topography of Alloy 22 Specimen After 35 Days Dripped at 80 °C [176 °F] and 85 Percent Relative Humidity: (a) Optical Micrograph, (b) 3-D Laser Scan Profiles of the Pit Area, and (c) 2-D Profiles

Note: The Square Box in (a) Indicates the Laser Scanning Area.

The Units in (b) and (c) Indicate x-, y-, z-axes Are Micrometer.

Because a part of the back side surface, except the areas inside the PTFE cylinder spacer, was wetted with the dripped water as seen in Figure 3-1(f), this wetted surface area of 11.19 cm^2 [1.73 in^2] was included in the exposed surface area.

As seen in Table 3-1, all samples exhibited weight loss and the amount of loss increased with test time. After 35 days, corrosion rate ranged from 78 to 96 nm/yr [3.07×10^{-6} to 3.78×10^{-6} in/yr] and the average rate was 85 nm/yr [3.35×10^{-7} in/yr] with the standard deviation of 7.98 nm/yr [3.14×10^{-7} in/yr]. This initially high corrosion rate is most likely due to the pit formation, resulting in large weight loss. However, corrosion rates gradually decreased with time. After 185 days of testing, Alloy 22 had an average corrosion rate of 25 nm/yr [9.84×10^{-7} in/yr]. Considering relatively shallow pits on the Alloy 22 surface after 185 days as demonstrated by surface topography, it is likely that existed pits could repassivate and no more pit propagation could occur. A decrease of Alloy 22 corrosion rate was generally observed as shown in Figure 1-1, and this was mainly due to the presence of the protective passive film formed on the Alloy 22 surface that inhibited fast metal dissolution.

3.1.2 Second Batch of Tests at 95 °C [203 °F] and Relative Humidity of 75 Percent

Figure 3-5 shows the posttest Alloy 22 specimens after 33 days of testing at 95 °C [203 °F] and relative humidity of 75 percent. Similar to the observations on Alloy 22 from the first batch, white deposits were also present on the specimens. By removing the deposits, as seen in Figure 3-6(a), the Alloy 22 surface exhibited several corrosion areas with tiny pits. Any changes

(a)
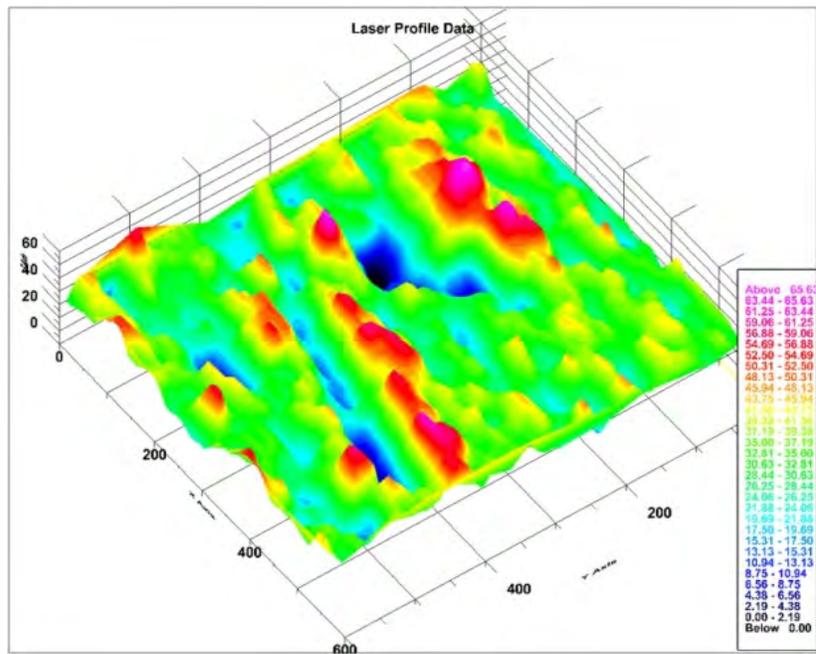
(b)

Figure 3-4. Surface Topography of Alloy 22 Specimen After 185 Days Dripped at 80 °C [176 °F] and 85 Percent Relative Humidity: (a) Optical Micrograph, (b) 3-D Laser Scan Profiles of the Pit Area, and (c) 2-D Profiles

Note: The Square Box in (a) Indicates the Laser Scanning Area.

The Units in (b) and (c) Indicates x-, y-, z-axes Are Micrometer.

Laser Line Profile Data
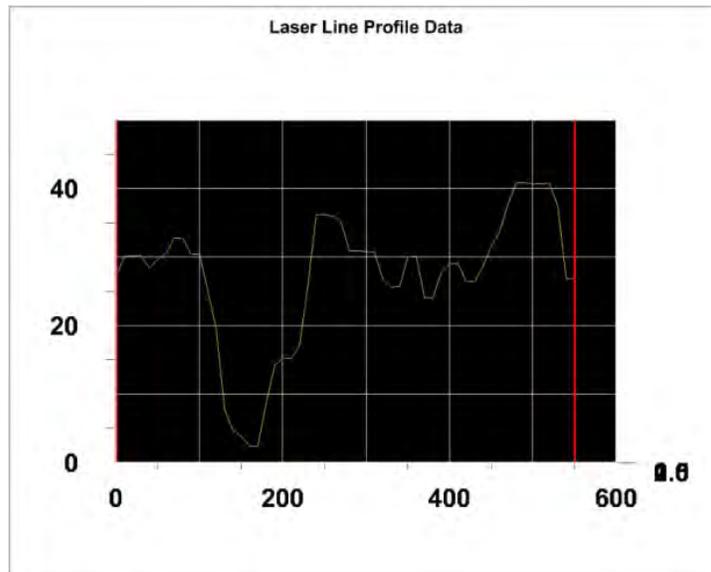
(c)

Figure 3-4 (continued). Surface Topography of Alloy 22 Specimen After 185 Days Dripped at 80 °C [176 °F] and 85 Percent Relative Humidity: (a) Optical Micrograph, (b) 3-D Laser Scan Profiles of the Pit Area, and (c) 2-D Profiles

Note: The Square Box in (a) Indicates the Laser Scanning Area.

The Units in (b) and (c) Indicates x-, y-, z-axes Are Micrometer.

Table 3-1. Corrosion Rates of Alloy 22 Dripped at 80 °C [176 °F] and 85 Percent Relative Humidity				
Specimen Identification (Dripping Duration)	Initial Weight (g)	Weight Loss (g)	Corrosion Rate (nm/yr)*	Average Corrosion Rate ± Standard Deviation (nm/yr)*
A (35 Days)	10.96570	0.00021	78	85 ± 7.98
B (35 Days)	10.99504	0.00026	96	
C (35 Days)	11.01710	0.00022	81	
D (35 Days)	11.08025	0.00023	85	
E (70 Days)	10.84316	0.00031	57	61 ± 5.23
F (70 Days)	10.98447	0.00035	61	
G (185 Days)	10.95778	0.00034	24	25 ± 1.48
H (185 Days)	10.96577	0.00037	26	
*1 nm/yr = 3.94 × 10^{-8} in/yr				
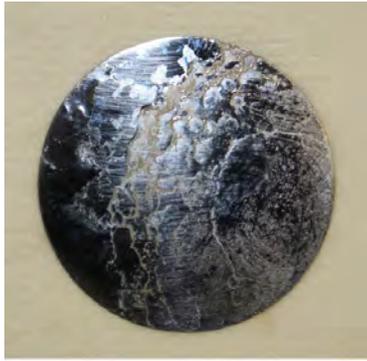
(a)   **(b)**

Figure 3-5. Photos of Posttest Surfaces of Alloy 22 After 33 Days Dripped at 95 °C [203 °F] and 75 Percent Relative Humidity for (a) Specimen I and (b) Specimen J
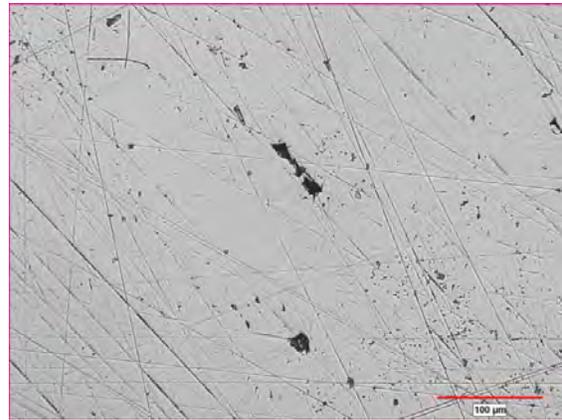
(a)   **(b)**

Figure 3-6. Optical Micrographs of Alloy 22 Surfaces Tested at 95 °C [203 °F] and 75 Percent Relative Humidity: (a) After 33 Days Dripped and (b) After 67 Days Dripped

in pit size and populations were not appreciable with of test time increased up to 67 days as shown in Figure 3-5(b), indicating no pit growth. Compared to the pits observed at a lower temperature of 80 °C [176 °F] from the first batch, interestingly, the size of pits at 95 °C [203 °F] was smaller.

Table 3-2 lists the calculation results of corrosion rates with weight losses after either 33 or 67 days of testing. The corrosion rate of 90 nm/yr [3.54×10^{-6} in/yr] for the 33-day tests decreased to 68 nm [2.68×10^{-6} in/yr] after 67 days of dripping. This decrease in corrosion rate with time is consistent with the tendency from the first batch; however, the corrosion rates at 95 °C [203 °F] were slightly higher those at 80 °C [176 °F], which could be due to the higher test temperature.

Table 3-2. Corrosion Rates of Alloy 22 Dripped at 95 °C [203 °F] and 75 Percent Relative Humidity				
Specimen Identification (Dripping Duration)	Initial Weight (g)	Weight Loss (g)	Corrosion Rate (nm/yr)*	Average Corrosion Rate ± Standard Deviation (nm/yr)*
I (33 Days)	10.25711	0.00020	78	90 ± 16.63
J (33 Days)	10.62251	0.00026	102	90 ± 16.63
K (67 Days)	9.67790	0.00025	48	68 ± 27.30
L (67 Days)	10.55815	0.00045	87	68 ± 27.30
*1 nm/yr = 3.94 × 10^{-8} in/yr				

3.1.3 Third Batch of Tests at 60 °C [140 °F] and Relative Humidity of 95 Percent

The third batch of tests was conducted at 60 °C [140 °F] and 95 percent relative humidity. Similar to the posttest specimens from the previous two batches, there was salt deposition on the Alloy 22 surface (see Figure 3-7). Salts were not strongly adhered to the specimen surface, while salts formed at both 80 and 95 °C [176 and 203 °F] were tightly adhered to the surface. Micrographs on the Alloy 22 surface after 32 days of testing revealed several corrosion pit areas along with many tiny pits as shown in Figure 3-8(a). The maximum size of the pits observed was about 10 μm [3.94 × 10^{-4} in] in width. After 60 days of testing, the pits tended to decrease in terms of size and amount, indicating repassivation of the pits. Consistent with the previous batches, with time, the corrosion rate decreased and reached the average rate of 24 nm/yr [9.45 × 10^{-7} in/yr] after 60 days of testing as shown in Table 3-3.

Figure 3-9 presents a comparison of the corrosion rates at temperatures of 60, 80, and 95 °C [140, 176, and 203 °F] as a function of time. As seen in the comparison, the corrosion rate was dependent on the test temperature in a dripped water environment. As the temperature increased, the corrosion rate increased. Compared to the corrosion rates of Alloy 22 in the literature (Sandia National Laboratories, 2007a), the range of corrosion rates measured at 80 and 95 °C [176 and 203 °F] under the simulated seepage water dripping condition in this study is close to the corrosion rates of Alloy 22 measured in an immersed condition at 90 °C [194 °F]. Note that the solutions used in the literature above were highly concentrated simulated water (e.g., saturated acidic water, saturated concentrated water, and basic saturated water). This result can also be valid within the test condition in this study in terms of range of temperature, humidity, and dripping rate.

3.1.4 Salt Chemistry Analysis

Thermodynamic Simulation of Solution Evaporation

Thermodynamic calculation was conducted using the OLI Analyzer Studio Version 3 code (Gerbino, 2006; OLI Systems, Inc., 2010) to determine the water chemistry and the salts that would result from evaporation of dripping water. Using the code's Mixed-Solvent Electrolyte chemistry option allows for simulation of aqueous chemical systems for temperatures up to 300 °C [572 °F], pressures up to 1,500 bar, and concentrations ranging from dilute conditions to pure molten salts or pure acids. Thermodynamic properties calculated with this software have been shown to agree very well with experimental data (e.g., Gruszkiewicz, et al., 2007). Of key interest was the concentration of aggressive species, such as chloride, and corrosion-inhibiting

species, such as nitrate. The chemical composition of the aqueous solution used in the Alloy 22 dripping tests was used as input in the evaporation simulation. This initially dilute water was evaporated to equilibrium using OLI Analyzer Studio at the following temperature and relative humidity conditions: (i) 60 °C [140 °F] and 95 percent relative humidity; (ii) 80 °C [176 °F] and 85 percent relative humidity; and (iii) 90 °C [203 °F] and 75 percent relative humidity. The compositions before and after evaporation are shown in Table 3-4. The OLI Analyzer Studio simulation indicated that the salts calcium carbonate, magnesium carbonate, sodium sulfate, and sodium–calcium sulfate would precipitate due to solution evaporation.

The calculated nitrate-to-chloride molar ratio of the evaporated solutions did not change from the initial value of 1.95. This value is a factor of 20 higher than the 0.1 value considered necessary to inhibit localized corrosion of Alloy 22 (Dunn, et al., 2003), which would imply Alloy 22 localized corrosion is not expected. However, the thermodynamic simulations assumed equilibrium conditions and therefore do not replicate the dynamic processes occurring in a corrosion test under dripping conditions. For example, evaporation on the Alloy 22 surface under dripping conditions could vary spatially and temporally. Transient processes could enable the less soluble sodium chloride to precipitate and the more soluble nitrate salts to remain dissolved in and flow with the transient solution. These processes would make the salts deposited on the Alloy 22 surface have nitrate-to-chloride ratios less than 0.1 and make the Alloy 22 material susceptible to localized corrosion. As discussed in the following section, EDS data suggest the presence of sodium chloride in the salt deposit but in amounts less than the detection limit of XRD analysis. Other dynamic processes of small water volume, temperature fluctuation, and mechanical (or chemical) impingement by water droplet may also affect the validity of the equilibrium thermodynamic simulation.

Salt Deposit Analysis

The chemical composition of the salts deposited on the Alloy 22 specimen was analyzed using EDS and XRD analysis. EDS was used to determine the elemental composition of the corrosion products, whereas XRD analysis was used to determine the structure and phases present. EDS analysis was carried out using a Noran Voyager M3105 system. XRD analysis was carried out using a Siemens Kristalloflex 805 with a D500 goniometer. The salts present in the corrosion products were identified by comparing the XRD spectroscopy of the samples with reference spectroscopy of different salts in a database. Note that XRD analysis has a detection limit of about 5 weight percent.

The EDS result is shown in Table 3-5, and the XRD data are shown in Figures 3-10 to 12. The XRD data indicate that the salts are dominantly calcium carbonate. Minor amounts of calcium sulfate, magnesium phosphate, calcium silicate carbonate, and magnesium silicate also could be present. The XRD result is consistent with the EDS data that show calcium and magnesium as the dominant elements in the salt deposit. Based on the EDS results, sodium chloride and sodium sulfate also could be present in the salt deposit but in amounts less than the detection limit of the XRD method. For comparison, OLI Analyzer Studio evaporation simulation indicated the possible formation of calcium carbonate, magnesium carbonate, sodium sulfate, and sodium-calcium sulfate.
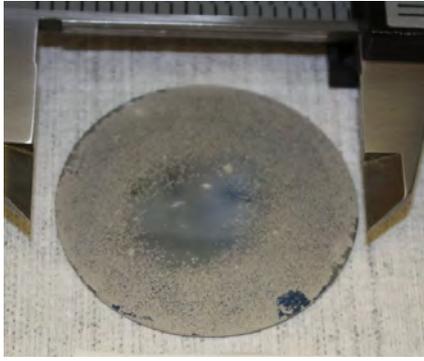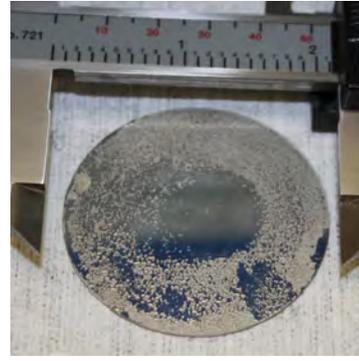
(a)   (b)

Figure 3-7. Photos of Posttest Surfaces of Alloy 22 After 60 Days Dripped at 60 °C [140 °F] and 95 Percent Relative Humidity for (a) Specimen Q and (b) Specimen R
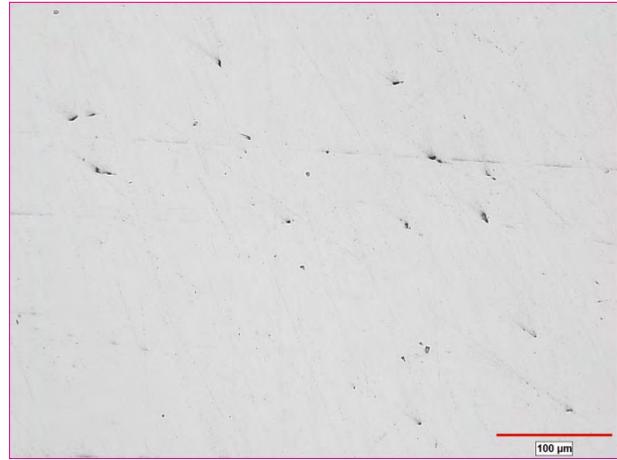
(a)   (b)

Figure 3-8. Optical Micrographs of Alloy 22 Surfaces Tested at 60 °C [140 °F] and 95 Percent Relative Humidity: (a) After 32 Days Dripped and (b) After 60 Days Dripped

Table 3-3. Corrosion Rates of Alloy 22 Dripped at 60 °C [140 °F] and 95 Percent Relative Humidity				
Specimen Identification (Dripping Duration)	Initial Weight (g)	Weight Loss (g)	Corrosion Rate (nm/yr)*	Average Corrosion Rate ± Standard Deviation (nm/yr)*
M (32 Days)	10.59580	0.00011	45	41 ± 12.20
N (32 Days)	10.20020	0.00007	29	
O (32 Days)	10.56262	0.00008	34	
P (32 Days)	10.47481	0.00014	57	
Q (60 Days)	10.23063	0.00013	28	24 ± 6.10
R (60 Days)	9.74089	0.00009	19	
*1 nm/yr = 3.94 × 10^{-8} in/yr				
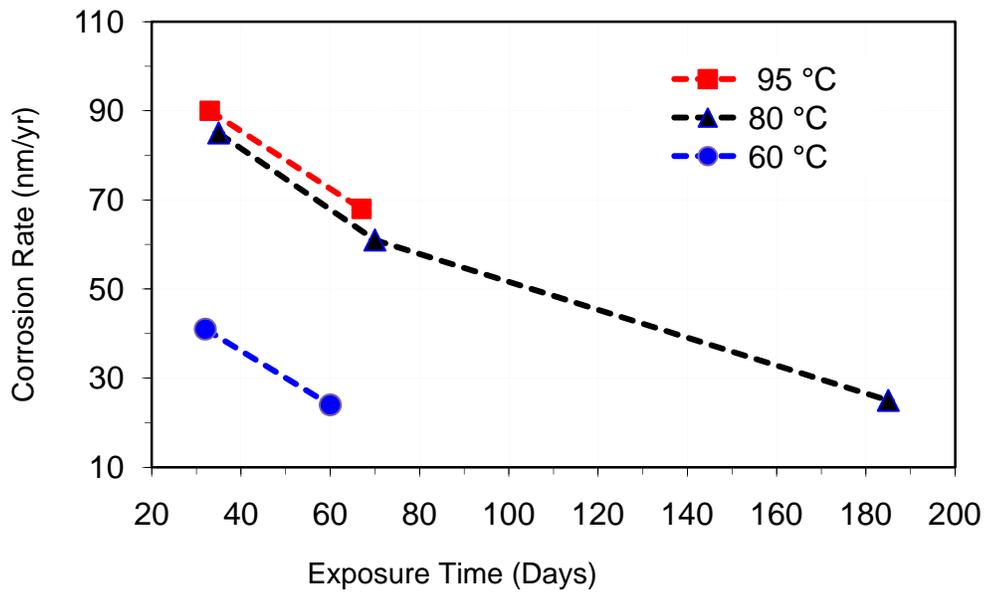
Figure 3-9. Corrosion Rate of Alloy 22 as a Function of Time Tested at Temperatures of 95, 80, and 60 °C [203, 176, and 140 °F]

Ionic Component	Concentration Before Evaporation* (molarity)	Concentration After Evaporation at 60 °C [140 °F] and 95 Percent Relative Humidity† (molarity)	Concentration After Evaporation at 80 °C [176 °F] and 85 Percent Relative Humidity† (molarity)	Concentration After Evaporation at 95 °C [203 °F] and 75 Percent Relative Humidity† (molarity)
Table 3-4. Solution Composition Before and After Evaporation				
Na$^+$	1.50×10^{-02}	$5.38 \times 10^{+00}$	$5.64 \times 10^{+00}$	$6.98 \times 10^{+00}$
K$^+$	1.70×10^{-04}	2.00×10^{-01}	3.24×10^{-01}	5.03×10^{-01}
Mg^{2+}	4.90×10^{-04}	6.13×10^{-02}	1.71×10^{-02}	6.15×10^{-03}
Ca^{2+}	9.90×10^{-04}	8.49×10^{-04}	4.40×10^{-04}	3.14×10^{-04}
Cl$^-$	7.70×10^{-04}	9.07×10^{-01}	$1.47 \times 10^{+00}$	$2.28 \times 10^{+00}$
SO$_4^{2-}$	7.00×10^{-03}	$1.51 \times 10^{+00}$	8.33×10^{-01}	3.88×10^{-01}
NO$_3^-$	1.50×10^{-03}	$1.77 \times 10^{+00}$	$2.86 \times 10^{+00}$	$4.44 \times 10^{+00}$
CO$_3^{2-}$	1.70×10^{-03}	3.45×10^{-04}	2.79×10^{-04}	1.55×10^{-04}
HCO$_3^-$	1.70×10^{-05}	1.70×10^{-02}	9.80×10^{-03}	5.23×10^{-03}
pH	—	7.70	7.62	7.47
NO$_3^-$/Cl$^-$ ratio	1.95	1.95	1.95	1.95

*Charge balanced using OLI Analyzer Studio
†Salts present after evaporation: CaCO$_3$, MgCO$_3$, Na$_2$SO$_4$, and Na$_2$Ca(SO$_4$)$_2$

Table 3-5. EDS Elemental Composition of Salt Deposit on Alloy 22 Specimen After 185 Days Dripped at 80 °C [176 °F] and 85 Percent Relative Humidity	
Element	Weight Percent
Na	0.45
Mg	2.68
Al	0.09
Si	0.71
P	0.16
S	0.60
Cl	1.45
Ca	93.86
Total	100.00
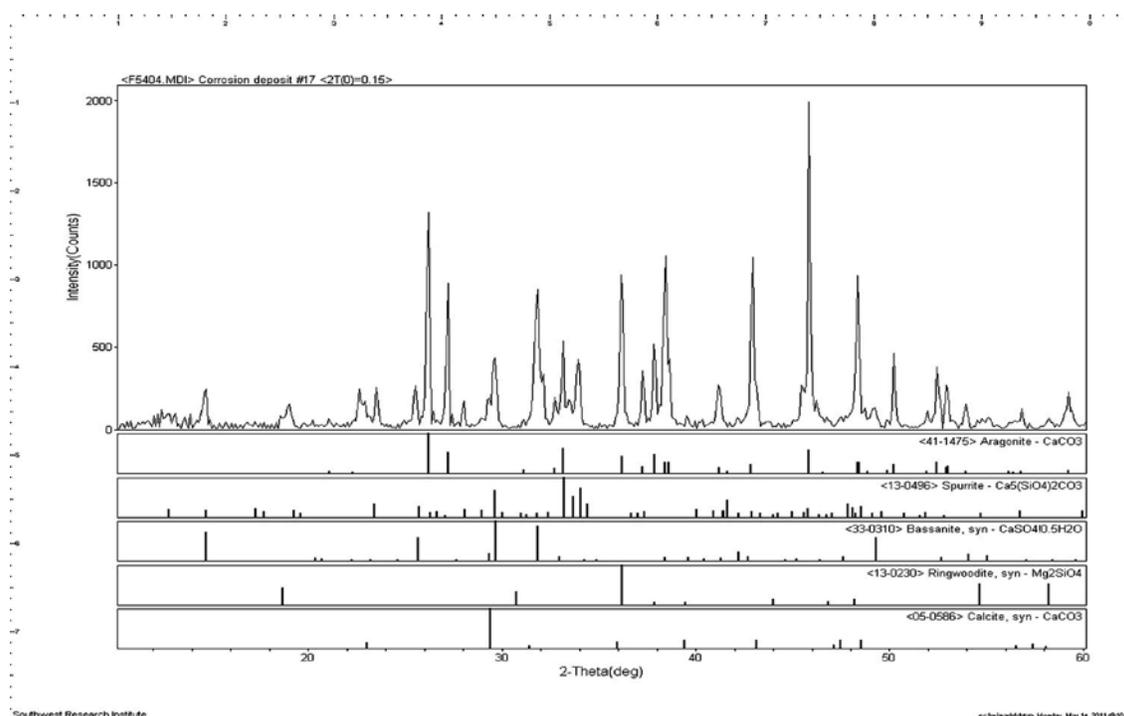
Figure 3-10. X-Ray Diffraction Spectroscopy of Salts Deposited on Alloy 22 Specimen After 32 Days Dripped at 60 °C [140 °F] and 95 Percent Relative Humidity. Also Shown Are the Reference Spectroscopy of Salts That Best Match the Salt Deposit Spectroscopy.
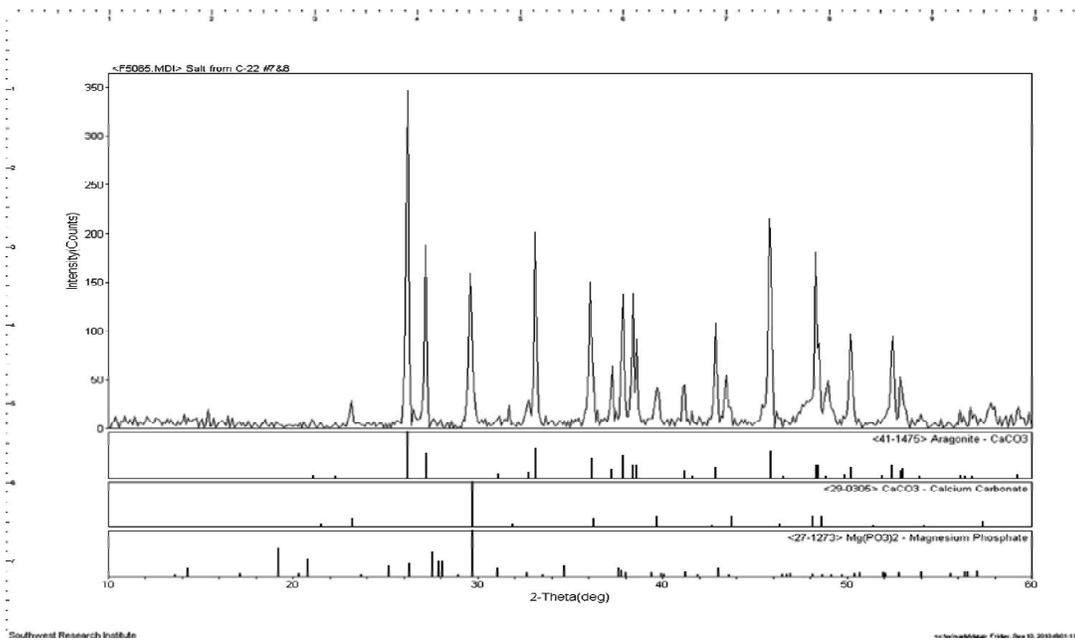
Figure 3-11. X-Ray Diffraction Spectroscopy of Salts Deposited on Alloy 22 Specimen After 185 Days Dripped at 80 °C [176 °F] and 85 Percent Relative Humidity. Also Shown Are the Reference Spectroscopy of Salts That Best Match the Salt Deposit Spectroscopy.
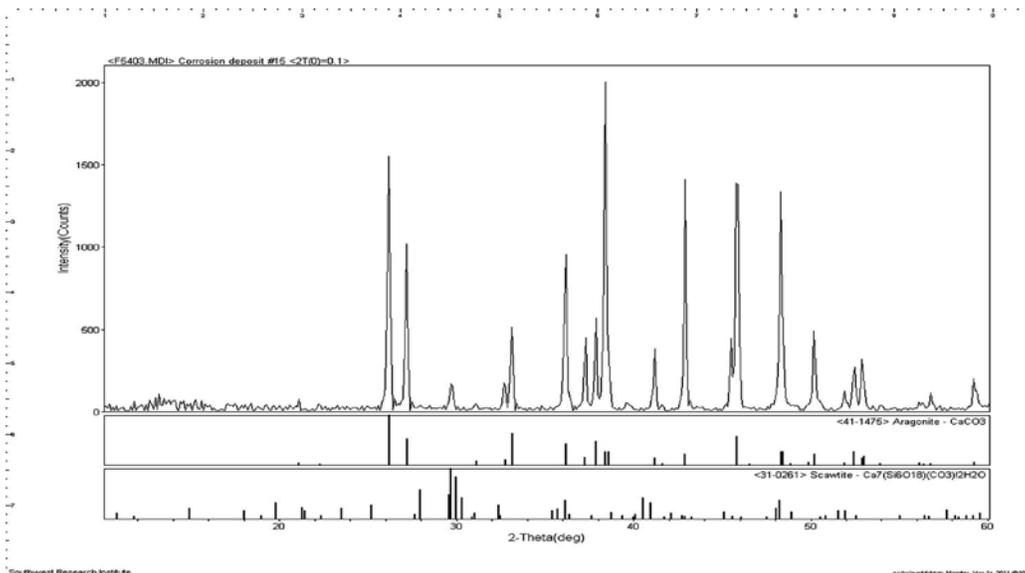
Figure 3-12. X-Ray Diffraction Spectroscopy of Salts Deposited on Alloy 22 Specimen After 67 Days Dripped at 95 °C [203 °F] and 75 Percent Relative Humidity. Also Shown Are the Reference Spectroscopy of Salts That Best Match the Salt Deposit Spectroscopy.

3.2 Titanium Alloys Dripping Test

3.2.1 First Batch of Tests at Temperature of 80 °C and Relative Humidity of 85 Percent

The first batch of tests was terminated after 181 days. Figure 3-13 shows the Titanium Grades 7 and 29 specimens after 6 months of testing at 80 °C [176 °F] and 85 percent relative humidity. The front side subjected to dripping was covered with a layer of white deposits. The back side, outside of the PTFE spacer covered area, was also covered with white deposits, but to a lesser extent. The white deposits were strongly adhered to the specimens, and they were not able to be removed by ultrasonic cleaning in deionized water. For both titanium Grades 7 and 29, the EDS in Figure 3-14 shows that the white deposits consist of calcium, carbon, oxygen, silicon, sulfur, aluminum, and magnesium. The higher concentration of calcium, carbon, and oxygen suggests that the white deposit is primarily $CaCO_3$, deposited from evaporation of the dripping water. Sulfur and magnesium came from the dripping water. Silicon and aluminum are likely from residual deposits from the specimen surface preparation process before the test or from trace elements in the chemicals used to prepare the dripping solution. No titanium or aluminum and vanadium were detected on the white deposits of Titanium Grade 7 or Grade 29 specimens, suggesting that the titanium corrosion product dissolved into the deposits was under the EDS detection limits.

The EDS in Figure 3-15 of the surface without deposits shows that there is a very small amount of carbon, magnesium, aluminum, silicon, and calcium deposited on the surface, but the main composition is the same as the original specimen without testing. For Titanium Grade 7, the palladium on the surface was not detectable by EDS. The specimen for comparison without being subjected to dripping shows a thin, multicolored corrosion layer (yellow, violet, and blue) likely because of optical interference colors caused by varying oxide film thickness.

All the specimens were chemically cleaned with HCl solution three times. Right after immersing the specimen in HCl solution, the white deposits dissolved and generated gas, which supports the previous assumption that the white deposits are primarily $CaCO_3$. Figure 3-16 shows the optical photos of the first HCl-cleaned specimens. Photos show that thick oxide still remained on the surface, and the weight difference summarized in Table 3-6 still showed weight gain after the test. After the third cleaning with HCl, the specimens were examined under the microscope with higher magnification, which showed consistently (as in Figure 3-17) that there is more general corrosion on the side subjected to dripping as evidenced by a smoother surface compared to more evident polishing scratches at the back side. Table 3-6 shows that the Titanium Grade 7 control specimen had negligible weight change, which suggests that the HCl solution cleaning does not dissolve the base metal. However, the Titanium Grade 29 specimen showed some weight loss, suggesting the dissolution of the base metal in HCl solution.

Because of the consistent weight gain after cleaning with HCl solution three times, the specimen was further cleaned in boiling 10 percent HNO_3 solution for 5 minutes per Covington and Schutz (1981). After the first cleaning with HNO_3, the specimens showed obvious weight loss compared to the specimen before the test, and the thick oxide shown in Figure 3-16 was cleaned away as shown in Figure 3-18. However, the Titanium Grade 7 control specimen also showed weight loss of about 0.2 mg [7×10^{-6} oz], which suggests that the HNO_3 solution slightly dissolved some base metals in addition to the corrosion products. Compared to Titanium Grade 7, the Titanium Grade 29 control specimen showed minimal weight change. All the specimens were further cleaned with HNO_3 solution, and showed very little weight change.

Specimens Subject to Dripping

Front Side

Back Side

Reference Specimens Without Dripping
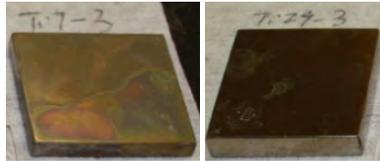
Figure 3-13. First Batch of Posttest Titanium Grades 7 and 29 Specimens at Temperature of 80 °C [176 °F] and Relative Humidity of 85 Percent. The specimen Size Was Approximately 4 × 4 × 0.6 cm^3 [1.6 × 1.6 × 0.2 in^3].
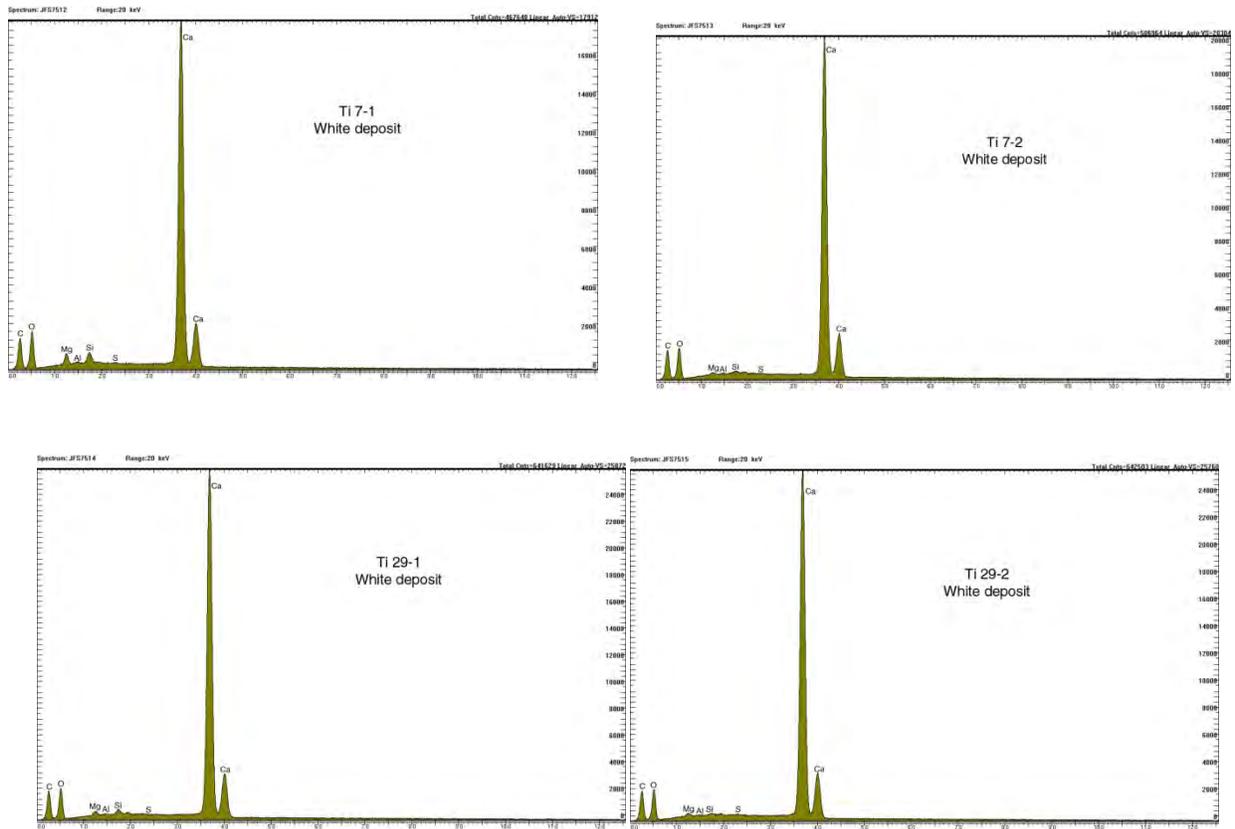
Figure 3-14. Energy-Dispersive X-Ray Spectroscopy of the White Deposits on the First Batch of Posttest Titanium Grades 7 and 29 Specimens Showing That the White Deposits Consist of Calcium, Carbon, Oxygen, Silicon, Sulfur, Aluminum, and Magnesium
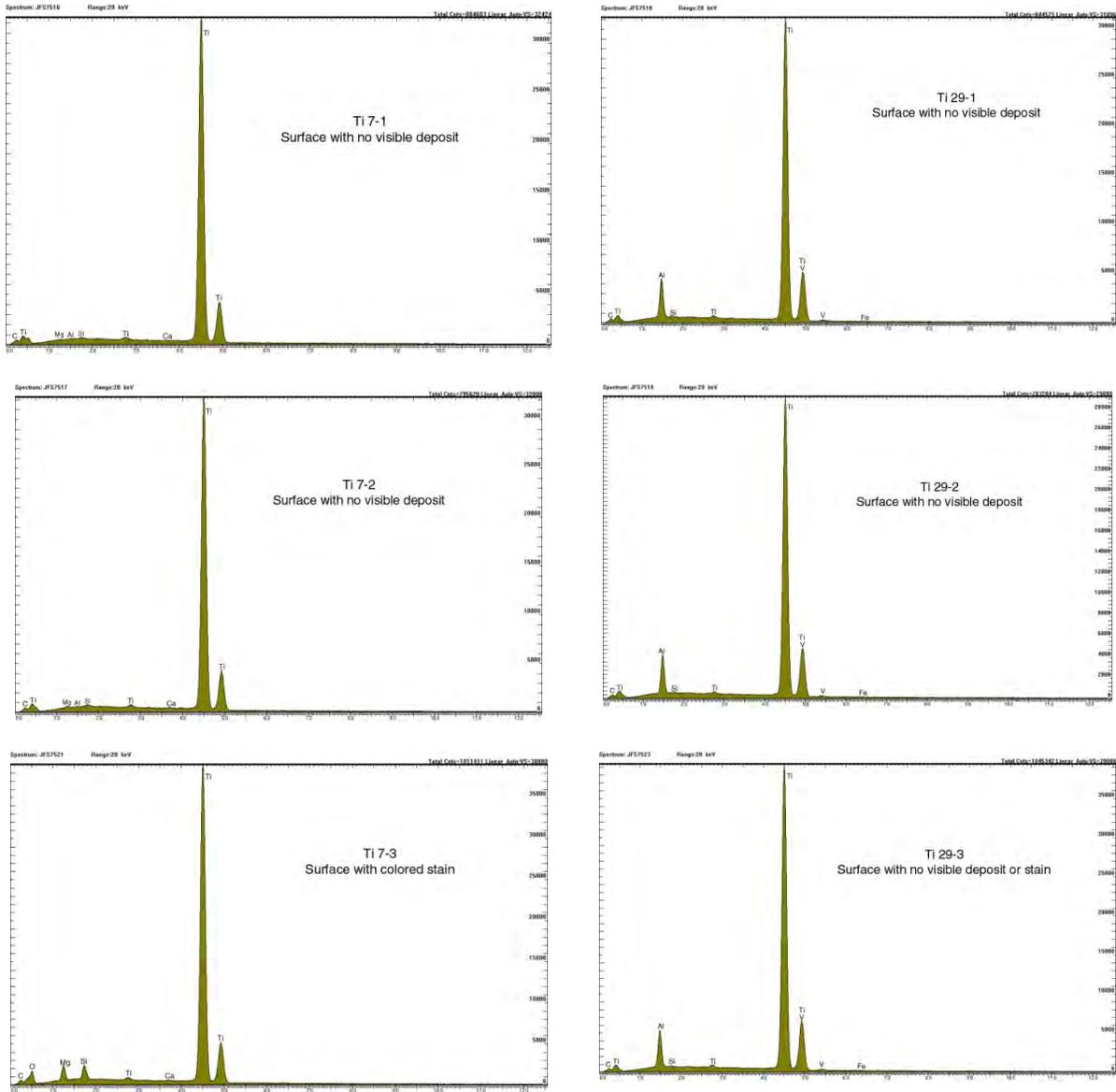
Figure 3-15. Energy-Dispersive X-Ray Spectroscopy of the First Batch of Posttest Titanium Grades 7 and 29 Specimen Surface Without Visible Deposits Showing the Main Constituent to be Elemental Titanium for Titanium Grade 7 and Titanium, Aluminum, and Vanadium for Titanium Grade 29.

After the removal of white deposits with HCl solution, the specimens were examined with a microscope along with the control specimen. For the tested specimens, there were some localized features protruding on the surface that persisted through the cleaning process. Similar features were shown on the control specimens. Figure 3-19 showed several examples of the localized features. Because both the tested and untested specimens showed similar features and these features were protruding from the surface, these features are not pits or any other localized corrosion form generated from the dripping process since they are features of the material in the as-received condition. They are considered to be artifacts of the manufacturing process or from the surface preparing process.
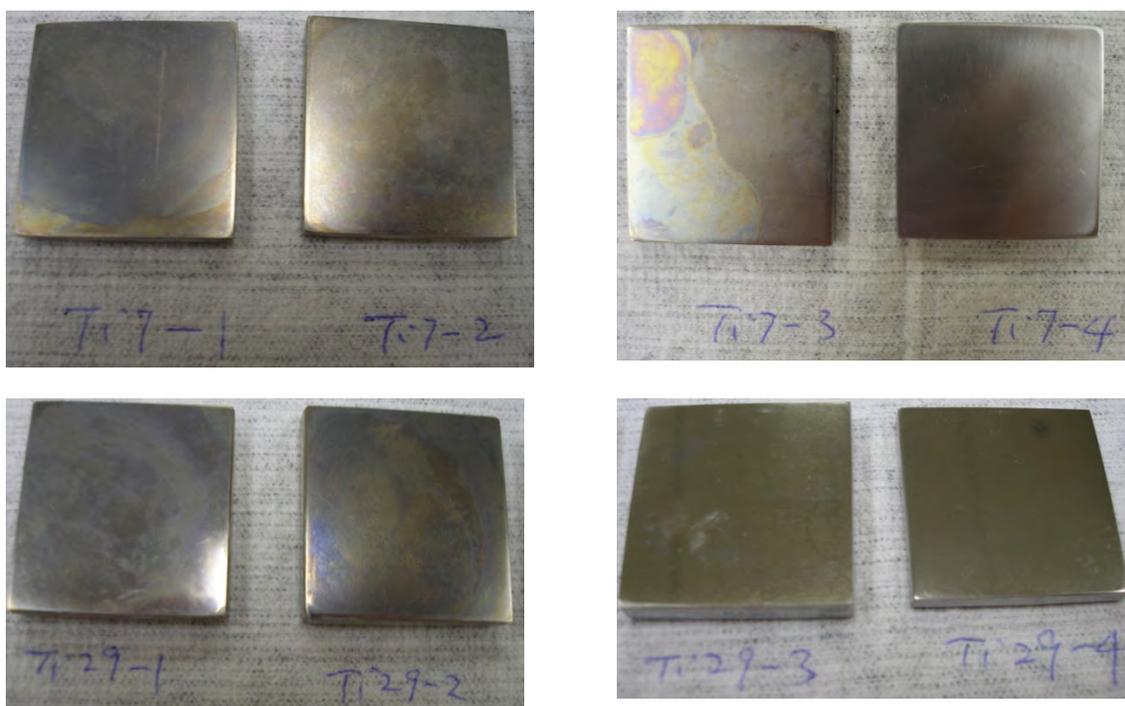
Figure 3-16. Optical Photos of the First Batch Posttest Specimens After Being Cleaned With HCl Solution Showing That All the White Deposits Were Cleaned, But the Thick Oxide Remained

Because further HNO_3 cleaning led to metal dissolution indicated by the control specimen, the weight loss to calculate the corrosion rate was determined from the weight difference of the specimen before the test and the first HNO_3 cleaning. The weight loss was not corrected by cleaning as recommended by ASTM G1–03 (ASTM International, 2003), although some weight loss was observed on the control specimens for the following reasons:

- The oxide film on the tested specimen was aged and thickened in the humidity chamber, while the oxide film on the control specimen was fresh and thin, possibly resulting in more dissolution of the control specimen in HCl. A simple correction by adding the weight loss from the control specimen to the weight loss of tested specimen may underestimate the actual weight loss of the test specimen.

- The corrosion rate calculated from weight loss without correction is more conservative.

The corrosion rate was calculated using Eq (3-1). For the specimens subject to dripping, the surface area is the entire surface area excluding the area covered by the PTFE cylinder. The material densities used for the calculation are 4.5 g/cm^3 [0.16 lb/in^3] for Titanium Grade 7 and 4.4 g/cm^3 [0.16 lb/in^3] for Titanium Grade 29. For the specimens subjected to dripping, the corrosion rates were in the range of 20–50 nm/yr [7.9 × 10^{-7}–2.0 × 10^{-6} in/yr], similar to what has been observed in literature data (Sandia National Laboratories, 2007b).

Ti 7-1 Front Side Subject to Dripping
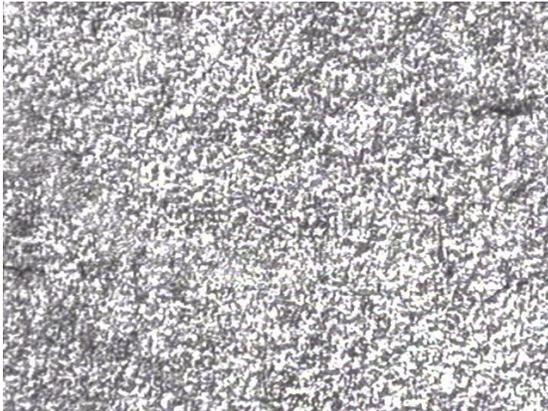
Ti 7-1 Back Side
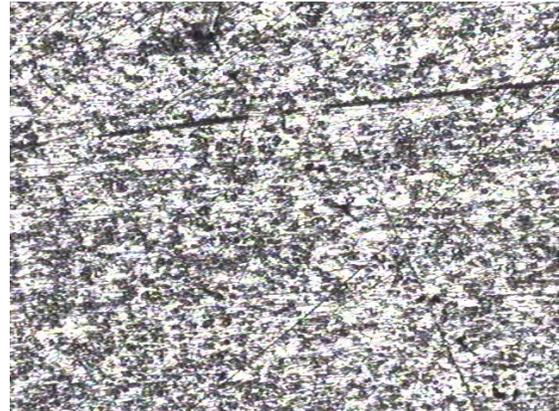
Ti 7-2 Front Side Subject to Dripping
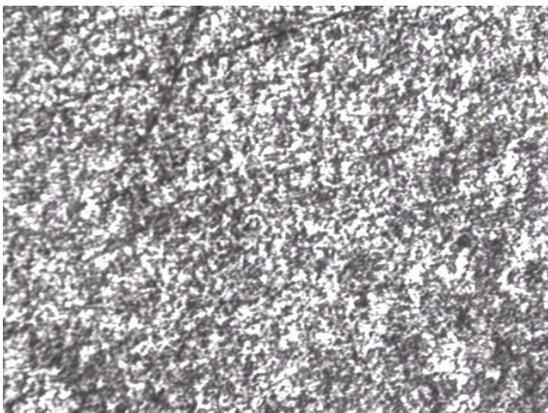
Ti 7-2 Back Side
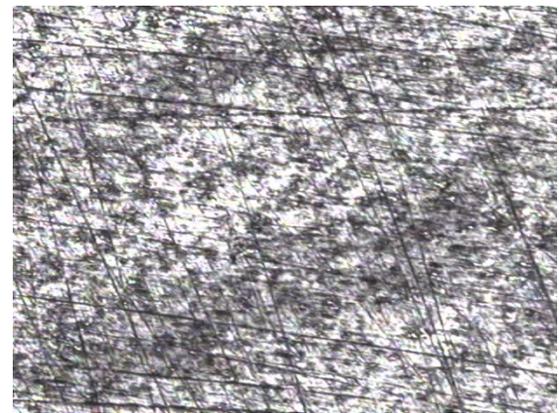
Ti 7-3 (Not Dripped Specimen) Front Side
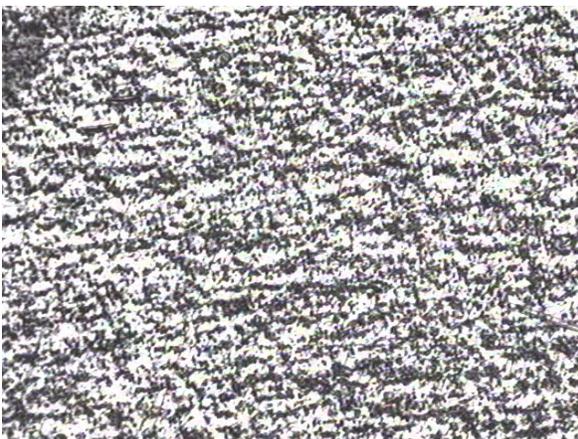
Ti 7-3 Back Side
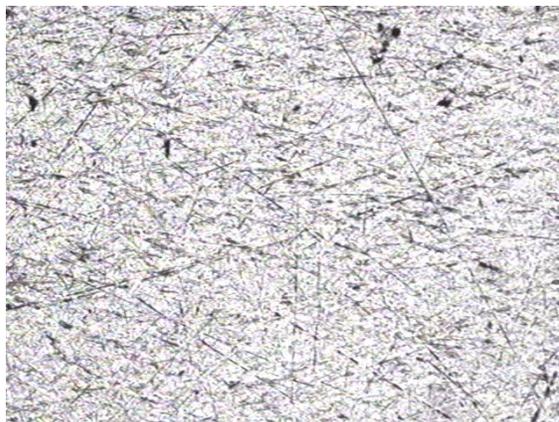
Figure 3-17. Surface of the Third HCl Cleaned Posttest Titanium Specimens Showing That the Dripping Side Was Corroded Uniformly and the Polishing Scratches Were Smoothed Out. However, There Was Less General Corrosion at the Back Side as Evidenced by the Polishing Scratches (Scale Bar Is Not Available, Because of the Limitation of the System).

Ti 29-1 Front Side Subject to Dripping

Ti 29-1 Back Side
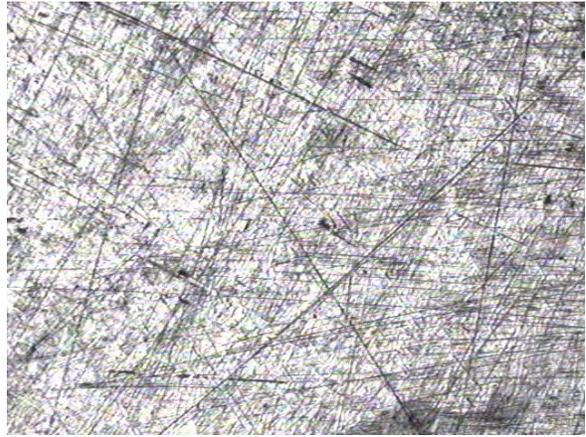
Ti 29-2 Front Side Subject to Dripping
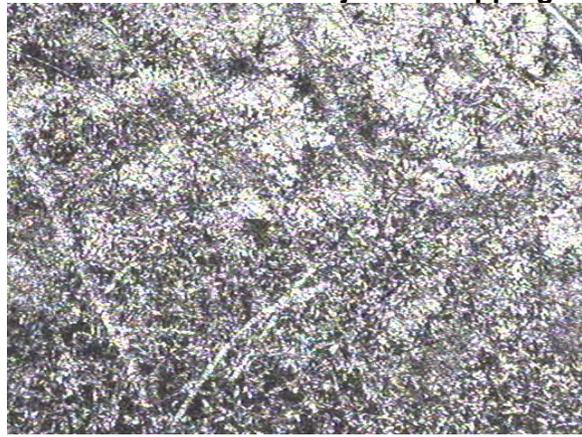
Ti 29-2 Back Side
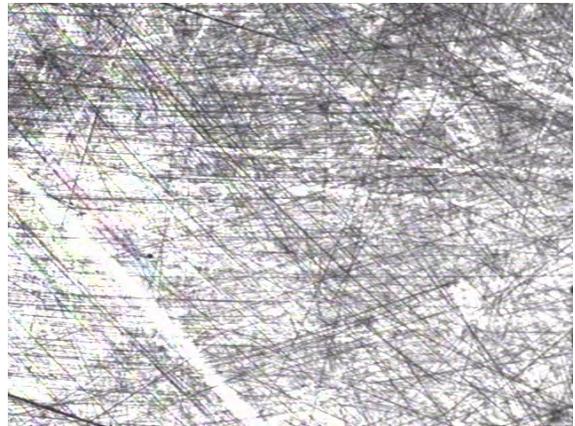
Ti 29-3 (Not Dripped Specimen) Front Side
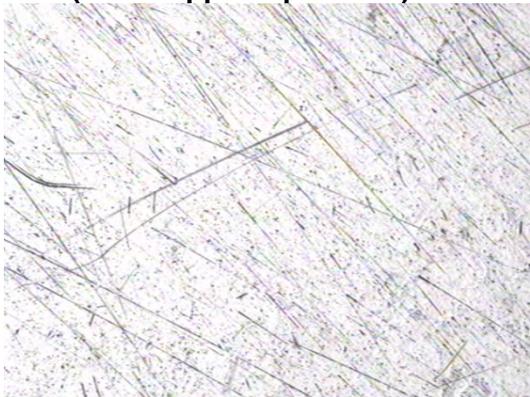
Ti 29-3 Back Side
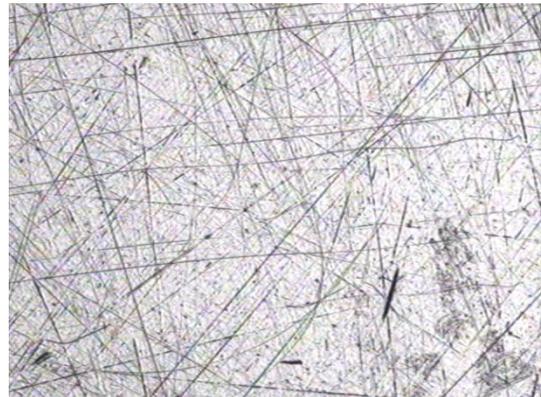
Figure 3-17 (continued). Surface of the Third HCl Cleaned Posttest Titanium Specimens Showing That the Dripping Side Was Corroded Uniformly and the Polishing Scratches Were Smoothed Out. However, There Was Less General Corrosion at the Back Side as Evidenced by the Polishing Scratches (Scale Bar Is Not Available, Because of the Limitation of the System).

Sample Identification	Ti 7-1	Ti 7-2	Ti 7-3 Without Dripping	Ti 7-4 (Control)	Ti 29-1	Ti 29-2	Ti 29-3 Without Dripping	Ti 29-4 (Control)
	Subject to Dripping				Subject to Dripping			
Initial weight, g	43.85001	42.33159	43.11402	42.58403	52.63078	53.48684	53.57979	34.33493
Posttest weight before acid cleaning, g	44.05787	42.57674	43.11535	N/A	52.83661	53.68799	53.57991	N/A
Weight gain after test, g	0.20786	0.24515	0.00133	N/A	0.20583	0.20115	0.00012	N/A
First HCl cleaning	43.85039	42.33199	43.11437	42.58402	52.63115	53.48718	53.57983	34.33492
Second HCl cleaning	43.85037	42.33199	43.11429	42.58403	52.63113	53.48712	53.57982	34.33502
Third HCl cleaning	43.85021	42.33188	43.11428	42.58403	52.63099	53.48697	53.57986	34.33475
First HNO$_3$ cleaning	43.84963	42.33132	43.11335	42.58380	52.63055	53.48649	53.57963	34.33472
Second HNO$_3$ cleaning	43.84965	42.33135	43.11329	42.58370	52.63046	53.48629	53.57954	34.33449
Weight loss, g	0.00038	0.00027	0.00067	N/A	0.00023	0.00035	0.00016	N/A
Corrosion rate, nm/yr	49.5	35.9	69.9	N/A	28.7	43.7	15.9	N/A

Table 3-6. First Batch Sample Weight Before and After Test at Temperature of 80 °C [176 °F] and Relative Humidity of 85 Percent

Titanium Grade 7 Front Side

Titanium Grade 7 Back Side

Titanium Grade 29 Front Side

Titanium Grade 29 Back Side

Figure 3-18. Optical Photographs of Specimens After First HNO$_3$ Solution Cleaning Showing That Most of the Corrosion Products Were Cleaned

Ti 7-1 Front Side Subject to Dripping
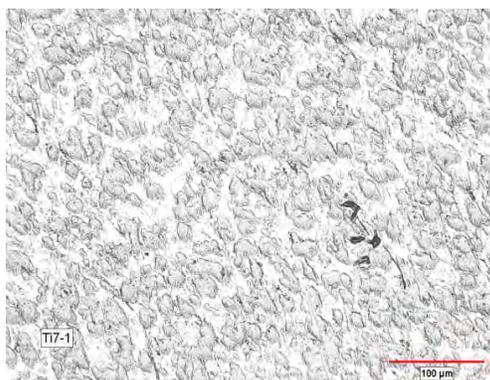
Ti 7-4 Untested Specimen
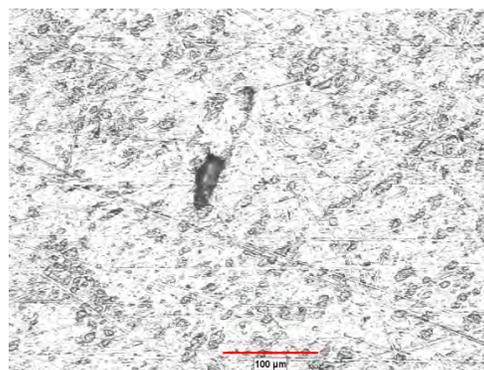
Ti 29-1 Front Side Subject to Dripping

Ti 29-4 Untested Specimen
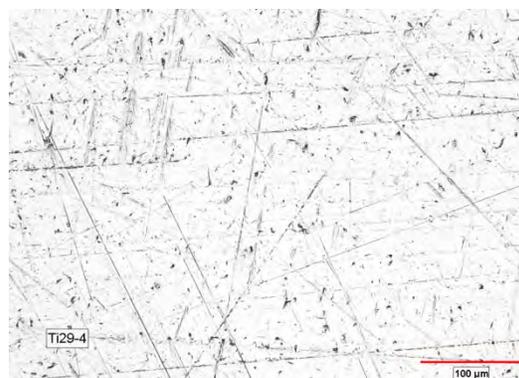
Figure 3-19. Optical Photographs of Second HNO₃-Cleaned Tested and Untested Specimens Showing That the Dripping Test Specimens Had Similar Features as the Untested Control Specimens. The Imperfections Shown on the Posttested Specimens Likely Existed Before the Test and Did Not Result From the Corrosion Process.

The Titanium Grade 7 specimen without dripping showed the highest corrosion rate, and the surface was covered by a colored surface film. This could be due to the relatively unstable environment near the edge of the humidity chamber.

3.2.2 Second Batch of Tests at Temperature of 95 °C [203 °F] and Relative Humidity of 75 Percent

The second batch of tests was terminated after 64 days. Figure 3-20 shows the posttest specimens. The specimens subject to dripping were covered with white deposits. EDS shows that the chemical composition is similar to that from the first batch of tests. The specimens without dripping showed some stains on the surface. Table 3-7 summarizes the weights before and after the test, the weight loss, and corrosion rates. All the specimens showed weight gain after the test because of the deposits and scales formed on the surface. After the first HCl cleaning, all the specimens subject to dripping still showed weight gain compared to the original

Subject to Dripping   **Subject to Dripping**

Without Dripping   **Without Dripping**

(a) Titanium Grade 7   **(b) Titanium Grade 29**
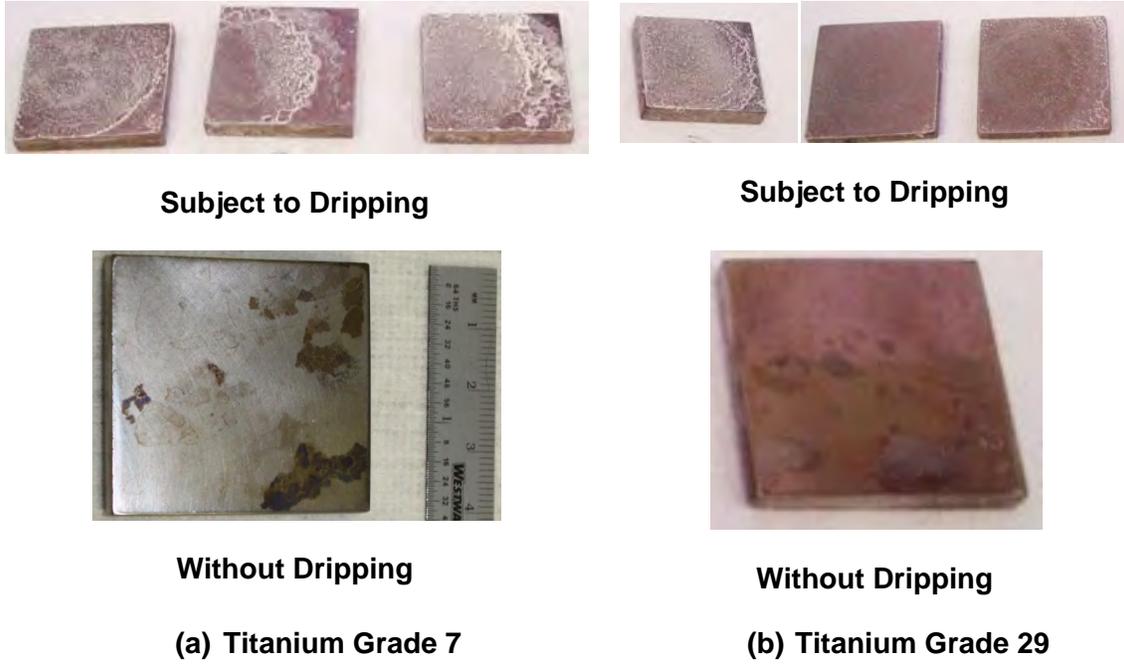
Figure 3-20. Second Batch of Posttest (a) Titanium Grade 7 and (b) Titanium Grade 29 Specimens at Temperature of 95 °C [203 °F] and Relative Humidity of 75 Percent

weight; the specimens without dripping showed weight loss. The control specimen also showed minor weight loss. All the specimens were examined under a microscope. No localized corrosion was observed. After the second HCl cleaning all the specimens showed weight loss compared to the original weight. It appears that the scales from the second batch of tests were easier to clean, possibly because of the shorter test duration. The control specimen also showed weight loss, possibly resulting from the dissolution of fresh oxide film on the surface compared to the aged surface film on the tested specimens. Because the control specimen consistently showed weight loss, the weight loss of the tested specimens was calculated based on the weight after the second HCl cleaning. This was compared to the original weight without correcting it from cleaning for reasons stated in Section 3.2.1. The corrosion rates were calculated based on Eq. (3-1) and shown in Table 3-7. The corrosion rates for Titanium Grades 7 and 29 under dripping were 130–380 nm/yr [5.12×10^{-6}–1.50×10^{-5} in/yr]

and 260–530 nm/yr [1.02×10^{-5}–2.09×10^{-5} in/yr], respectively, higher than what was measured from the first batch of tests. The higher corrosion rates could be caused by the shorter test duration and higher test temperature.

	Table 3-7. Second Batch Sample Weight Before and After Tests at Temperature of 95 °C [203 °F] and Relative Humidity of 75 Percent									
	Titanium Grade 7					**Titanium Grade 29**				
Samples	**Subject to Dripping**			**Without Dripping**	**Control Specimen**	**Subject to Dripping**			**Without Dripping**	**Control Specimen**
Initial weight, g	42.97176	42.36883	42.63832	42.62994	41.01415	53.31863	33.63283	34.32682	34.14560	51.52964
Posttest weight before acid cleaning, g	43.02630	42.40567	42.73694	42.63050	N/A	53.34756	33.66642	34.43903	34.14598	N/A
Weight gain after test, g	0.05454	0.03684	0.09862	0.00056	N/A	0.02893	0.03359	0.11221	0.00038	N/A
First HCl cleaning	42.97266	42.37071	42.63862	42.62974	41.01387	53.31882	33.63344	34.32722	34.14561	51.52942
Second HCl cleaning	42.97075	42.36847	42.63741	42.62832	41.01251	53.31715	33.63197	34.32613	34.14311	51.52795
Weight loss, g	0.00101	0.00036	0.00091	0.00162	N/A	0.00148	0.00086	0.00069	0.00249	N/A
Corrosion rate, nm/yr	372	133	336	473	N/A	521	333	267	755	N/A

4   CONCLUSIONS

In this report, the corrosion behavior of Alloy 22 and Titanium Grades 7 and 29 was evaluated under seepage water dripping conditions. Three batches of dripping tests were conducted on Alloy 22 and two batches of tests were conducted on Titanium Grades 7 and 29. The following are the main conclusions from this study.

Corrosion of Alloy 22

- In the first batch of tests at 80 °C [176 °F] and 85 percent relative humidity, the surfaces of the posttest specimens exhibited several corrosion pits along with many small sized pits. After 185 days of testing, the pits appeared to be shallow and there was no clear evidence of pit propagation. The corrosion rate decreased with test duration, and the measured rate was 25 nm/yr [9.84×10^{-7} in] after 185 days' exposure.

- In the second batch at 95 °C [203 °F] and 75 percent relative humidity, pits were also present on the specimen surface. However, with time, the corrosion rate decreased. At a low temperature of 60 °C [140 °F] and relative humidity of 95 percent in the third batch test, the corrosion rate decreased with time and reached 24 nm/yr [9.45×10^{-7} in] after 60 days of testing. There was no evidence of pit propagation.

- Under the seepage water dripping condition, Alloy 22 exhibited a temperature-dependent corrosion rate, which was commonly observed in the immersion tests. The corrosion rates obtained from the dripping tests in this study were close to the rates obtained from immersion tests in the literature.

- Results of the salt chemistry analyses through thermodynamic calculations and analysis tools indicate that major composition was calcium carbonate; several other compositions were possibly precipitated, including magnesium carbonate, sodium (calcium) sulfate, sodium chloride, and silica.

Corrosion of Titanium Alloys

- The first batch of tests at 80 °C [176 °F] and 85 percent relative humidity for 181 days showed that the corrosion rates of the specimens subjected to dripping were in the range of 20–50 nm/yr [7.9×10^{-7}–2.0×10^{-6} in/yr], similar to data obtained in immersion tests in the literature. No clear difference was observed between Titanium Grades 7 and 29. The front side subjected to direct dripping corroded more than the back side that was not subjected to direct dripping.

- The second batch of tests at 95 °C [203 °F] and 75 percent relative humidity for 64 days showed that the corrosion rates for Titanium Grades 7 and 29 under dripping were 130–380 nm/yr [5.12×10^{-6}–1.50×10^{-5} in/yr] and 260–530 nm/yr [1.02×10^{-5}–2.09×10^{-5} in/yr], respectively, higher than what was measured from the first batch of tests. The higher corrosion rates could be caused by the shorter test duration and higher test temperature.

- No localized corrosion was observed on either material from the two batches of tests.

5 REFERENCES

Ashida, Y., L.G. McMillion, and M. Misra. "Communication C: A Heated Electrode Test System for Studying Corrosion Behavior of Alloy 22." *Nuclear Waste Research: Siting, Technology and Treatment*. A.P. Lattefer, ed. Hauppauge, New York: Nova Science Publishers, Inc. pp. 25–36. 2008.

ASTM International. "Standard Specification for Titanium and Titanium Alloy Strip, Sheet, and Plate." ASTM B265–07. West Conshohocken, Pennsylvania: ASTM International. 2008.

_____. "Standard Specification for Titanium and Titanium Alloy Seamless Pipe." ASTM B861–10. West Conshohocken, Pennsylvania: ASTM International. 2010.

_____. "Preparing, Cleaning, and Evaluating Corrosion Test Specimens." ASTM G1–03. West Conshohocken, Pennsylvania: ASTM International. 2003.

Bechtel SAIC Company, LLC. "General Corrosion and Localized Corrosion of the Drip Shield." ANL–EBS–MD–000004. Rev 02. Las Vegas, Nevada: Bechtel SAIC Company, LLC. 2004.

Covington, L.C. and R.W. Schutz. "Resistance of Titanium to Atmospheric Corrosion." Proceedings of the Corrosion 81 Conference. Paper No 113. Houston, Texas: NACE International. 1981.

Dunn, D.S., Y.-M. Pan, X. He, L.T. Yang, and R.T. Pabalan. "Evolution of Chemistry and Its Effects on the Corrosion of Engineered Barrier Materials." The 30th Symposium on the Scientific Basis for Nuclear Waste Management Materials Research Society 2006 Fall Meeting, Boston, Massachusetts November 27–December 1, 2006. Pittsburgh, Pennsylvania: Materials Research Society. 2006.

Gerbino, A. "A Guide for Using the OLI Analyzers." Morris Plains, New Jersey: OLI Systems, Inc. 2006.

Gruszkiewicz, M.S., D.A. Palmer, R.D. Springer, P. Wang, and A. Anderko. "Phase Behavior of Aqueous Na–K–Mg–Ca–Cl–NO3 Mixtures: Isopiestic Measurements and Thermodynamic Modeling." *Journal of Solution Chemistry*. Vol. 36. pp. 723–765. 2007.

Kursten, B., E. Smailos, I. Azkarate, L. Wermer, N.R. Smart, and G. Santarini. "COBECOMA, State-of-the-Art Document on the Corrosion Behavior of Container Materials." Contract N FIKW-CT-20014-20138 Final Report. Burssels, Belgium: European Commission. 2004.

Lin, C., B. Leslie, R. Codell, H. Arlt, and T. Ahn. "Potential Importance of Fluoride to Performance of the Drip Shield." Proceedings of the American Nuclear Society 10th International High-Level Radioactive Waste Management Conference, Las Vegas, Nevada, March 30–April 2, 2003, La Grange Park, Illinois: American Nuclear Society. 2003.

OLI Systems, Inc. "A Guide to Using OLI Analyzer Studio Version 3.1." Morris Plains, New Jersey: OLI Systems, Inc. 2010.

Sandia National Laboratories. "Total System Performance Assessment Model/Analysis for the License Application." MDL–WIS–PA–000005. Rev 00 AD 01, ERD 3. Las Vegas, Nevada: Sandia National Laboratories. 2008a.

_____. "Multiscale Thermohydrologic Model." ANL–EBS–MD–000049. Rev. 03, ADD 02 ERD 1. Las Vegas, Nevada: Sandia National Laboratories. 2008b.

_____. "General Corrosion and Localized Corrosion of Waste Package Outer Barrier." ANL–EBS–MD–000003. Rev 03. Las Vegas, Nevada: Sandia National Laboratories. 2007a.

_____. "General Corrosion and Localized Corrosion of the Drip Shield." ANL–EBS–MD–000004. Rev 02. AD 01. Las Vegas, Nevada: Sandia National Laboratories. 2007b.

Schutz, R.W. "Platinum Metal Additions to Titanium: A Highly Effective Strategy for Enhancing Corrosion Resistance." *Corrosion*. Vol. 59. pp. 1,043–1,057. 2003.

Schutz, R.W. "Corrosion of Titanium and Titanium Alloys." ASM Handbook. Vol. 13B. *Corrosion*: Materials. Materials Park, Ohio: ASM International. 2005.

Sedriks, A.J. "Corrosion Resistance of Titanium-Ruthenium Alloys." *Corrosion*. Vol. 31. pp. 60–65. 1975.